Published for SISSA by Springer

Received: October 10, 2013
Revised: December 4, 2013
Accepted: December 27, 2013
Published: January 20, 2014

Higgs boson mass, neutrino masses and mixing and keV dark matter in an $U(1)_R-$ lepton number model

Sabyasachi Chakraborty and Sourov Roy

Department of Theoretical Physics, Indian Association for the Cultivation of Science, 2A & 2B Raja S.C. Mullick Road, Jadavpur, Kolkata-700032, India

E-mail: tpsc3@iacs.res.in, tpsr@iacs.res.in

Abstract: We discuss neutrino masses and mixing in the framework of a supersymmetric model with an $U(1)_R$ symmetry, consisting of a single right handed neutrino superfield with an appropriate R charge. The lepton number (L) of the standard model fermions are identified with the negative of their R-charges. As a result, a subset of leptonic R-parity violating operators can be present and are consistent with the $U(1)_R$ symmetry. This model can produce one light Dirac neutrino mass at the tree level without the need of introducing a very small neutrino Yukawa coupling. We analyze the scalar sector of this model in detail paying special attention to the mass of the lightest Higgs boson. One of the sneutrinos might acquire a substantial vacuum expectation value leading to interesting phenomenological consequences. Different sum rules involving the physical scalar masses are obtained and we show that the lightest Higgs boson mass receives a contribution proportional to the square of the neutrino Yukawa coupling f. This allows for a 125 GeV Higgs boson at the tree level for $f \sim \mathcal{O}(1)$ and still having a small tree level mass for the active neutrino. In order to fit the experimental results involving neutrino masses and mixing angles we introduce a small breaking of $U(1)_R$ symmetry, in the context of anomaly mediated supersymmetry breaking. In the presence of this small R-symmetry breaking, light neutrino masses receive contributions at the one-loop level involving the R-parity violating interactions. We also identify the right handed neutrino as a warm dark matter candidate in our model. In the case of R-symmetry breaking, the large f case is characterized by a few hundred MeV lightest neutralino as an unstable lightest supersymmetric particle (LSP) and we briefly discuss the cosmological implications of such a scenario.

Keywords: Supersymmetry Phenomenology

ArXiv ePrint: 1309.6538

doi:10.1007/JHEP01(2014)101

Contents

JHEP01(2014)101

1 Introduction

The observation of a new neutral boson, widely believed to be the first elementary scalar boson of nature, by the CMS and ATLAS experimental collaborations at the CERN LHC is perhaps the most important discovery in high energy physics in recent times [1, 2]. The mass of this particle is measured to be $\sim 125\,\text{GeV}$. Obviously, more data and analysis can confirm whether this is the Higgs boson of the standard model (SM) or not. On the other hand, supersymmetric particle searches by ATLAS and CMS for pp collision at center-of-mass energy, $\sqrt{s} = 7$ and $8\,\text{TeV}$, has observed no significant excess over the expected SM background. This has set stringent limits on the superparticle masses (particularly on the masses of squarks and gluinos) for a number of supersymmetric models/scenarios [3, 4].

At the same time, we have very strong experimental evidences in favor of neutrino oscillation [5–7]. These results have firmly established the existence of massive neutrinos and non-trivial mixing pattern in the neutrino sector (including the recent discovery [8, 9] of a small but non-zero mixing angle θ_{13}). Non-vanishing neutrino masses and mixing are very important indications of new physics. Naturally, the neutrino sector is a testing ground for various models going beyond the SM.

There is also compelling evidence for the existence of dark matter (DM) and cosmological observations have measured the relic density of DM with a high degree of precision [10, 11]. Nevertheless, the identity of the DM remains unknown to date and the potential candidates are, for example, the lightest neutralino in an R-parity conserving supersymmetric theory, the gravitino, the axino, the axion and the keV sterile neutrino [12].

On the theoretical side, supersymmetry (SUSY) is a very popular choice for new physics. The minimal supersymmetric standard model (MSSM) with R-parity violation (RPV) is an intrinsically supersymmetric way of generating observed neutrino masses and mixing pattern. There are extensive studies involving MSSM with R-parity violation on neutrino masses and mixing, under various assumptions, both at the tree and the loop level [13].

It is, therefore, tempting to see whether there exist supersymmetric models which can naturally explain the observed mass of the new scalar boson at $\sim 125\,\text{GeV}$, relax the strong constraints on SUSY particle masses coming from the LHC, provide a suitable dark matter candidate and at the same time produce neutrino masses and mixing consistent with current data. In this direction a class of very interesting models are those with a global continuous $\text{U}(1)_R$ symmetry [14–18]. Models with R-symmetry have Dirac gauginos instead of Majorana gauginos and the bounds on the first two generation squarks are somewhat relaxed compared to MSSM because of the presence of a Dirac gluino [19–32]. Flavor and CP violating constraints are also suppressed in this class of models [33].

Let us mention at this stage that extensive studies have been performed with Dirac gaugino masses in the R-symmetric limit. In order to have a Dirac gaugino mass [29], one needs to incorporate a singlet superfield $\hat{S}$ in the adjoint representation of $\text{U}(1)_Y$, an $\text{SU}(2)_L$ triplet superfield $\hat{T}$ (with zero hypercharge), and an $\text{SU}(3)_C$ octet superfield $\hat{O}$. The Dirac gaugino masses have also been motivated from "supersoft" supersymmetry breaking [34]. Another notable feature of these models are, the absence of trilinear scalar

JHEP01(2014)101

interactions (*A terms*) and also the μ term, when the R-symmetry is preserved. However one can reintroduce these terms by considering the breaking of R-symmetry [35].

Recently, there have been very interesting proposals where the $U(1)_R$ symmetry was identified with the lepton number [14–18]. A classification of phenomenologically interesting R-symmetric models has been performed in ref. [16] showing that leptonic or baryonic RPV operators are allowed by such R-symmetries. The role of the down type Higgs is played by the sneutrino in these models, which can acquire a significant vacuum expectation value (vev) and a light Higgs boson with a mass of $\sim 125\,\text{GeV}$ can be produced [14–16, 18]. If lepton number is identified with the $U(1)_R$ symmetry then even in the presence of leptonic RPV operators one cannot generate neutrino Majorana masses violating lepton number by two units ($\Delta L = 2$). One way to avoid such a problem is to introduce light Dirac neutrino masses involving gauge singlet neutrino superfields with appropriate R-charges.

In this work we take a very interesting and minimalistic approach and introduce only a single right handed neutrino superfield in the model. We shall discuss in detail at a later stage that this model can produce one very light Dirac neutrino[1] at the tree level with an Yukawa coupling as large as $\sim 10^{-4}$ and in some cases even with an Yukawa coupling of $\mathcal{O}(1)$. In the presence of only a single right-handed neutrino the low energy spectrum includes two massless neutrinos and one must think of some other mechanism to generate non-zero mass to at least one of these massless neutrinos. This can be achieved by introducing a small breaking of $U(1)_R$ symmetry. We know that a non-zero gravitino mass $m_{3/2}$ implies breaking of $U(1)_R$ symmetry. In this work we shall consider a small gravitino mass $m_{3/2} \lesssim 10\,\text{GeV}$ in the context of anomaly mediated supersymmetry breaking. This ensures that the effects of $U(1)_R$ symmetry breaking are also not very large. In fact, the small breaking of R-symmetry generates small Majorana masses for the gauginos as well as trilinear scalar interactions or the A-terms [15]. We shall show in our subsequent analysis that these small R-breaking parameters will induce non-zero Majorana mass terms for the neutrinos at the tree level as well as at the one-loop level. Moreover, gravitino mass in this ballpark is also consistent with primordial nucleosynthesis, thermal leptogenesis and gravitino as a cold dark matter candidate [36].

Our analysis shows that in the case of a large neutrino Yukawa coupling f, an additional tree level contribution to the lightest CP-even Higgs boson mass can be obtained, which can be significant for a value of $f \sim \mathcal{O}(1)$. Note that even with such a large value of f one can have a small active neutrino mass at the tree level. In the presence of this large f the lightest neutralino with a large bino component and having a mass of a few hundred MeV becomes the LSP. The long-lived gravitino (with a mass $m_{3/2} \sim$10 GeV) is the next-to-lightest supersymmetric particle (NLSP) and in order to be cosmologically consistent this requires a reheating temperature $T_R \lesssim 10^6\,\text{GeV}$.

One important thing to note is that in this model we can have a sterile neutrino with mass of the order of a few keV. This can be identified as a warm dark matter candidate [37] with appropriate relic density. We have checked that the active sterile mixing is small and

[1] Although the generic feature of this model would be to have a relatively heavy Dirac neutrino, by appropriate tuning of some parameters one can have a Dirac neutrino mass less than 0.1 eV or so.

JHEP01(2014)101

consistent with the experimental observations of satellite based X-ray telescopes. Thus we are able to have a situation, where appropriate values of light neutrino masses and mixing angles are achieved along with a warm dark matter candidate in the form of sterile neutrino.

The plan of the paper is as follows. First in section 2, we give an introduction to the $U(1)_R$ symmetric model with one right handed neutrino superfield. Section 3 describes the scalar sector of this model along with the electroweak symmetry breaking conditions. The generation of a $\sim 125\,\text{GeV}$ Higgs boson mass through one loop radiative corrections is discussed in some detail. The neutrino sector in R-symmetric case is discussed in section 4. We introduce R-symmetry breaking in section 5 in the framework of anomaly mediated supersymmetry breaking. Neutrino masses at the tree level are discussed in detail accompanied by necessary analytical results. In section 6 we consider the possibility of having a eV scale sterile neutrino in this model and discuss its incompatibility to explain the LSND [38–40] anomaly. Next we present our discussion of a keV scale sterile neutrino as a warm dark matter candidate in section 7. Section 8 describes the contribution to neutrino mass matrix at the one-loop level in the R-symmetry breaking scenario. We present a comprehensive discussion on the results of our numerical analysis of neutrino masses and mixing and keV dark matter in section 9, along with the constraints on RPV couplings as a function of the gravitino mass. The case of large neutrino Yukawa coupling and its relation to the tree level Higgs boson mass is discussed in section 10. We conclude in section 11 along with future outlook.

2 $U(1)_R$ model with a right handed neutrino

We consider a minimal extension of the model, introduced in [16], with the standard MSSM superfields $\hat{H}_u$, $\hat{H}_d$, $\hat{Q}_i$, $\hat{U}_i^c$, $\hat{D}_i^c$, $\hat{L}_i$, $\hat{E}_i^c$ ($i = 1, 2, 3$), along with one right handed neutrino superfield $\hat{N}^c$. In addition to this, vector like $SU(2)_L$ doublet superfields $\hat{R}_u$ and $\hat{R}_d$, with opposite hypercharge ($Y = 1, -1$ respectively) are considered. These doublets, with appropriate R charge assignments, were originally introduced in order to have an anomaly free framework [33] and they are inert in nature. The reason for this inertness is, if $\hat{R}_u$ and $\hat{R}_d$ acquires a vev, the R-symmetry will be broken spontaneously, which we would like to avoid. Again, as mentioned earlier, the bino and wino do not possess Majorana masses in the R-symmetry preserving scenario. However, they can acquire Dirac masses and for that one has to consider superfields in the adjoint representation of the standard model gauge group. These superfields are, a singlet $\hat{S}$, a triplet $\hat{T}$, under $SU(2)_L$ (with zero hypercharge), and an octet $\hat{O}$, under $SU(3)_c$. For example, by pairing the singlet $\hat{S}$, with the bino, one obtains a Dirac bino mass term and so on.

As discussed in ref. [15, 16], we identify the R-symmetry with lepton number symmetry in such a way that the lepton numbers of the SM fermions are identified with the negative of their R-charges whereas the superpartners of the SM fermions carry lepton numbers same as their R-charges. Below we make a table of different superfields in this model with their appropriate R-charges.

JHEP01(2014)101

	$\hat{Q}_i$	$\hat{U}_i^c$	$\hat{D}_i^c$	$\hat{L}_i$	$\hat{E}_i^c$	$\hat{H}_u$	$\hat{H}_d$	$\hat{R}_u$	$\hat{R}_d$	$\hat{S}$	$\hat{T}$	$\hat{O}$	$\hat{N}^c$
$\mathrm{U}(1)_R$	1	1	1	0	2	0	0	2	2	0	0	0	2

Table 1. $\mathrm{U}(1)_R$ charge assignments to the superfields.

The superpotential in the R-preserving case becomes,

$$\begin{aligned} W = & y^u_{ij}\hat{H}_u\hat{Q}_i\hat{U}^c_j + \mu_u\hat{H}_u\hat{R}_d + f_i\hat{L}_i\hat{H}_u\hat{N}^c + \lambda_S\hat{S}\hat{H}_u\hat{R}_d + 2\lambda_T\hat{H}_u\hat{T}\hat{R}_d - M_R\hat{N}^c\hat{S} \\ & + \mu_d\hat{R}_u\hat{H}_d + \lambda'_S\hat{S}\hat{R}_u\hat{H}_d + \lambda_{ijk}\hat{L}_i\hat{L}_j\hat{E}^c_k + \lambda'_{ijk}\hat{L}_i\hat{Q}_j\hat{D}^c_k + 2\lambda'_T\hat{R}_u\hat{T}\hat{H}_d \\ & + y^d_{ij}\hat{H}_d\hat{Q}_i\hat{D}^c_j + y^e_{ij}\hat{H}_d\hat{L}_i\hat{E}^c_j + \lambda_N\hat{N}^c\hat{H}_u\hat{H}_d. \end{aligned} \tag{2.1}$$

Here the triplet $\hat{T}$ under $\mathrm{SU}(2)_L$, is parametrised as [41, 42],

$$\begin{aligned} \hat{T} &= \sum_{a=1,2,3} \hat{T}^{(a)}, \\ &= \frac{1}{2}\begin{pmatrix} \hat{T}_0 & \sqrt{2}\hat{T}_+ \\ \sqrt{2}\hat{T}_- & -\hat{T}_0 \end{pmatrix}, \end{aligned} \tag{2.2}$$

where $\hat{T}^{(a)} = T_a\frac{\sigma^a}{2}$, σ^a's are the Pauli matrices and we denote $T_3 = T_0$, $T_+ = \frac{1}{\sqrt{2}}(T_1 - iT_2)$ and $T_- = \frac{1}{\sqrt{2}}(T_1 + iT_2)$. Note that the most general superpotential contributing to the renormalizable interactions in the Lagrangian includes other terms such as

$$W' = \kappa\hat{N}^c\hat{S}\hat{S} + \eta\hat{N}^c. \tag{2.3}$$

However, in this work for simplicity we will keep κ and η to be equal to zero. It is also important to note that a term of the type $\mu^i_L\hat{R}_u\hat{L}_i$ can, in principle, be added to the superpotential. Nevertheless, one can rotate away this term using a redefinition of the superfields $\hat{L}_i$ and $\hat{H}_d$ such that only a linear combination of these superfields couples to $\hat{R}_u$ in the superpotential, which we identify as the new $\hat{H}_d$. One must remember that the above superpotential (eq. (2.1)) is written in this rotated basis.

2.1 Soft supersymmetry breaking interactions

The R-symmetric model discussed above must contain supersymmetry breaking in order to make a realistic phenomenological model. In order to do this we have to imagine that supersymmetry breaking is not associated with R-symmetry breaking in the global supersymmetry case. This can be achieved by including both D-term supersymmetry breaking as well as F-term supersymmetry breaking [16, 43]. Introducing the spurion superfields $W'_\alpha = \lambda'_\alpha + \theta_\alpha D'$, the Dirac gaugino mass terms appear in the Lagrangian as

$$\mathcal{L}^{\text{Dirac}}_{\text{gaugino}} = \int d^2\theta\frac{W'_\alpha}{\Lambda}\left[\sqrt{2}\kappa_1\ W_{1\alpha}\hat{S} + 2\sqrt{2}\kappa_2\ \mathrm{tr}(W_{2\alpha}\hat{T}) + 2\sqrt{2}\kappa_3\ \mathrm{tr}(W_{3\alpha}\hat{O})\right] + \text{h.c.} \tag{2.4}$$

The terms written in eq. (2.4) preserve a $\mathrm{U}(1)_R$ symmetry under which the $W_{i\alpha}$ and W'_α have R-charge 1. Accordingly, $\mathrm{R}[\lambda_{i\alpha}] = \mathrm{R}[\lambda'_\alpha] = 1$ and $\mathrm{R}[D'] = 0$.

JHEP01(2014)101

The integration over the Grassmann coordinates generates the Dirac gaugino mass terms as

$$\mathcal{L}^{\rm Dirac}_{\rm gaugino} = -M_1^D \lambda_1 \tilde{S} - M_2^D \lambda_{2i} \tilde{T}_i - M_3^D \lambda_{3a} \tilde{O}_a + \ldots, \tag{2.5}$$

where $M_j^D = \kappa_j D'/\Lambda$ are the Dirac gaugino masses with $j = 1, 2, 3$ corresponding to the $\mathrm{U}(1)_Y$, $\mathrm{SU}(2)_L$, and $\mathrm{SU}(3)_C$ gauge groups respectively. Here Λ is the scale at which SUSY breaking is mediated and $\hat{S}$, $\hat{T}$, and $\hat{O}$ are the chiral superfields in the adjoint representation of the gauge groups as mentioned earlier, with

$$\begin{aligned} \hat{S} &= S + \sqrt{2}\theta\tilde{S} + \ldots, \\ \hat{T} &= T + \sqrt{2}\theta\tilde{T} + \ldots, \\ \hat{O} &= O + \sqrt{2}\theta\tilde{O} + \ldots \end{aligned} \tag{2.6}$$

The $\mathrm{U}(1)_R$ conserving soft supersymmetry breaking terms in the scalar sector are generated by the spurion superfield $\hat{X}$ defined as $\hat{X} = x + \theta^2 F_X$, (with $\langle x \rangle = 0$, $\langle F_X \rangle \neq 0$, $\mathrm{R}[\hat{X}] = 2$), and can be written as

$$\begin{aligned} V_{\rm soft} =\ & m_{H_u}^2 H_u^\dagger H_u + m_{R_u}^2 R_u^\dagger R_u + m_{H_d}^2 H_d^\dagger H_d + m_{R_d}^2 R_d^\dagger R_d + m_{\tilde{L}_i}^2 \tilde{L}_i^\dagger \tilde{L}_i + m_{\tilde{R}_i}^2 \tilde{l}_{Ri}^\dagger \tilde{l}_{Ri} \\ & + M_N^2 \tilde{N}^{c\dagger} \tilde{N}^c + m_S^2 S^\dagger S + 2m_T^2 \mathrm{tr}(T^\dagger T) + 2m_O^2 \mathrm{tr}(O^\dagger O) + (B\mu H_u H_d + \mathrm{h.c.}) \\ & - (b\mu_L^i H_u \tilde{L}_i + \mathrm{h.c.}) + (t_S S + \mathrm{h.c.}) + \frac{1}{2} b_S (S^2 + \mathrm{h.c.}) + b_T (\mathrm{tr}(TT) + \mathrm{h.c.}) \\ & + B_O (\mathrm{tr}(OO) + \mathrm{h.c.}). \end{aligned} \tag{2.7}$$

We neglect the $\mathrm{U}(1)_R$ symmetric scalar trilinear terms in the expression in eq. (2.7) because they are assumed to be suppressed by the factor $m_{\rm SUSY}/\Lambda$ where $m_{\rm SUSY} \sim 1\,\mathrm{TeV}$ and Λ is typically much larger than $m_{\rm SUSY}$ [16]. It has been argued in ref. [44] that the dangerous t_S parameter in scenarios with Dirac gaugino masses are suppressed and that is what we shall consider in the present work, so that this term does not introduce quadratic divergence leading to phenomenological disaster. Note that the tadpole term $(t_{\tilde{N}^c} \tilde{N}^c + \mathrm{h.c.})$ is absent from the scalar potential because of R-symmetry.

The presence of the bilinear term $b\mu_L^i H_u \tilde{L}^i$ in the scalar potential can, in general, lead to non-zero vevs[2] (v_i, $i = 1, 2, 3$) for all the three left-handed sneutrinos. However, we can still rotate to a basis in which only one of the left-handed sneutrinos acquires a non-zero vev. The rotation can be defined as [13]

$$\hat{L}_i = \frac{v_i}{v_a} \hat{L}_a + e_{ib} \hat{L}_b, \tag{2.8}$$

where $\hat{L}_a$ is the combination of the $\hat{L}_i$ superfields whose neutral scalar component gets a non-zero vev v_a, $a = 1(e)$ whereas the other sneutrino fields corresponding to $\hat{L}_b$, $b =$

[2] In this model sneutrino vevs do not violate lepton number and hence they are not constrained from the consideration of small Majorana neutrino masses of active neutrinos.

JHEP01(2014)101

2, 3(μ, τ) do not acquire any vacuum expectation value, that is to say $v_b = 0$ for $b =$ 2, 3(μ, τ). Here $v_a \equiv \sqrt{\sum_i v_i^2}$ and the superfield $\hat{L}_a$ is defined as

$$\hat{L}_a = \frac{1}{v_a} \sum_i v_i \hat{L}_i. \tag{2.9}$$

The vectors $\{e_{i2}\}$ and $\{e_{i3}\}$ are orthogonal to each other and normalized to unity. In addition, they are also orthogonal to the vector $\{v_i\}$.

In this basis the term $f_i \hat{L}_i \hat{H}_u \hat{N}^c$ in the superpotential transforms into $\frac{f_i v_i}{v_a} \hat{L}_a \hat{H}_u \hat{N}^c + f_i e_{ib} \hat{L}_b \hat{H}_u \hat{N}^c$. Using the freedom to choose f_i such that $f_i e_{ib} = 0$, the modified neutrino Yukawa coupling term in the superpotential looks like $f \hat{L}_a \hat{H}_u \hat{N}^c$, where $f \equiv \frac{f_i v_i}{v_a}$. Therefore, in this rotated basis the right handed neutrino superfield $\hat{N}^c$ couples only with $\hat{L}_a$, $a = 1(e)$ with a coupling strength f. Note that in this single sneutrino vev basis the soft supersymmetry breaking bilinear term in the scalar potential involving the doublet slepton field and the $\hat{H}_u$ field appears as $\epsilon^{ij} b \mu_L^a H_u^i \tilde{L}_a^j$ + h.c. [$a = 1(e)$], where $\{i,\ j\}$ are SU(2) indices with $\epsilon^{12} = -\epsilon^{21} = 1$. The model can be made even more minimal by integrating out the fields $\hat{R}_u$ and $\hat{H}_d$, as discussed in [16]. This is the situation when the left-handed sneutrino vev $\langle \tilde{\nu}_1 \rangle$ is much greater[3] than the down-type Higgs vev $\langle H_d^0 \rangle$ and can be achieved with $\mu_d^2 \gg m_{\tilde{L}}^2$ where μ_d is the coefficient of the bilinear term $\mu_d \hat{R}_u \hat{H}_d$ in the superpotential and $m_{\tilde{L}}^2$ is the soft mass squared of the left-handed sleptons. In such a case the masses of the charged lepton and down type quarks arise because of the non-zero vev of the left-handed sneutrino.

Furthermore, the trilinear RPV interactions in the superpotential looks like

$$\begin{aligned} \frac{1}{2}\lambda_{ijk} \hat{L}_i \hat{L}_j \hat{E}_k^c + \lambda'_{ijk} \hat{L}_i \hat{Q}_j \hat{D}_k^c = & \sum_{b=2,3} \frac{v_i e_{jb}}{v_a} \lambda_{ijk} \hat{L}_a \hat{L}_b \hat{E}_k^c + \lambda'_{ijk} \frac{v_i}{v_a} \hat{L}_a \hat{Q}_j \hat{D}_k^c \\ & + \frac{1}{2}(e_{ib} e_{jc} \lambda_{ijk}) \hat{L}_b \hat{L}_c \hat{E}_k^c + \sum_{b=2,3} e_{ib} \lambda'_{ijk} \hat{L}_b \hat{Q}_j \hat{D}_k^c. \end{aligned} \tag{2.10}$$

From eq. (2.10) we can identify the Yukawa couplings and the trilinear R-parity violating couplings in the single sneutrino vev basis as,

$$f_{bk}^l = \sum_{ij} \frac{v_i e_{jb}}{v_a} \lambda_{ijk}, \qquad f_{jk}^d = \sum_i \frac{v_i}{v_a} \lambda'_{ijk}, \tag{2.11}$$

$$\lambda_{bck} = \sum_{ij} e_{ib} e_{jc} \lambda_{ijk}, \qquad \lambda'_{bjk} = \sum_i e_{ib} \lambda'_{ijk}. \tag{2.12}$$

In the basis where the charged lepton ($\hat{L}_b$, $b = 2, 3$) and down type Yukawa couplings are diagonal, the above superpotential given in eq. (2.10) can be re-written as

$$\begin{aligned} W^{\rm diag} = & \sum_{b=2,3} f_b^l \hat{L}_a \hat{L}'_b \hat{E}'^c_b + \sum_{k=1,2,3} f_k^d \hat{L}_a \hat{Q}'_k \hat{D}'^c_k \\ & + \sum_{k=1,2,3} \frac{1}{2} \tilde{\lambda}_{23k} \hat{L}'_2 \hat{L}'_3 \hat{E}'^c_k + \sum_{j,k=1,2,3;b=2,3} \tilde{\lambda}'_{bjk} \hat{L}'_b \hat{Q}'_j \hat{D}'^c_k. \end{aligned} \tag{2.13}$$

[3]The constraints on the sneutrino vev can be obtained from the precision electroweak measurements of the vector and axial-vector coupling of the Z boson to charged leptons as well as from the measurements of tau lepton Yukawa coupling [14, 16].

JHEP01(2014)101

Here the prime on the lepton ($\hat{L}'_b,\ b=2,3$) and quark superfields denotes that they are in the mass-eigenstate basis[4] and $\tilde{\lambda},\ \tilde{\lambda}'$ are the trilinear R-parity violating couplings in that basis. In our subsequent analysis we shall work in this mass eigenstate basis and remove the prime from the fields along with $\tilde{\lambda},\ \tilde{\lambda}' \to \lambda,\ \lambda'$. Remember that we are also working in a basis where only one left-handed sneutrino (corresponding to flavor a) gets a vev. To reiterate, we observe that these trilinear RPV operators are consistent with the R-symmetric superpotential. Nevertheless, this superpotential conserves lepton number because of the identification of lepton number with R-charges and hence the lepton number violating processes do not constrain these trilinear couplings. The flavor structures of these trilinear R-parity violating couplings in this model will have important implications in the context of neutrino masses and other phenomenology as we shall discuss later.

In view of the above discussion it is easy to see that the superpotential and the soft SUSY breaking scalar potential include the following terms

$$W = y^u_{ij}\hat{H}_u\hat{Q}_i\hat{U}^c_j + \mu_u\hat{H}_u\hat{R}_d + f\hat{L}_a\hat{H}_u\hat{N}^c + \lambda_S\hat{S}\hat{H}_u\hat{R}_d + 2\lambda_T\hat{H}_u\hat{T}\hat{R}_d - M_R\hat{N}^c\hat{S} + W^{\rm diag}, \quad (2.14)$$

and

$$\begin{aligned} V_{\rm soft} =\ & m^2_{H_u}H^\dagger_u H_u + m^2_{R_d}R^\dagger_d R_d + m^2_{\tilde{L}_a}\tilde{L}^\dagger_a\tilde{L}_a + \sum_{b=2,3} m^2_{\tilde{L}_b}\tilde{L}^\dagger_b\tilde{L}_b + M^2_{\tilde{N}}\tilde{N}^{c\dagger}\tilde{N}^c \\ & + m^2_{\tilde{R}_i}\tilde{l}^\dagger_{Ri}\tilde{l}_{Ri} + + m^2_S S^\dagger S + 2m^2_T{\rm tr}(T^\dagger T) + 2m^2_O{\rm tr}(O^\dagger O) - (b\mu_L H_u\tilde{L}_a + {\rm h.c.}) \\ & + (t_S S + {\rm h.c.}) + \frac{1}{2}b_S(S^2 + {\rm h.c.}) + b_T({\rm tr}(TT) + {\rm h.c.}) + B_O({\rm tr}(OO) + {\rm h.c.}) \quad (2.15) \end{aligned}$$

With the above superpotential and the soft SUSY breaking scalar potential, in the R-symmetry conserving scenario, we would now like to analyze the scalar sector of this model consisting of the CP-even neutral scalars, CP odd neutral scalars and the charged scalars in detail. Here we assume that no CP violating phases exist in the scalar potential.

3 The scalar sector

The scalar potential comprises of four different terms.

$$V = V_F + V_D + V_{\rm soft} + V_{\rm one-loop}, \quad (3.1)$$

where V_F is the F-term contribution to the scalar potential, V_D is the D-term contribution, $V_{\rm soft}$ is the soft supersymmetry breaking part and $V_{\rm one-loop}$ is the one-loop contribution to

[4]Note, however, that the mass of the lepton of flavor a cannot be generated from the trilinear R-parity violating operators and one must invoke R-symmetry preserving supersymmetry breaking operators to generate a small mass.

JHEP01(2014)101

the scalar potential. The relevant part of the F-term contribution is,

$$\begin{aligned}
V_F &= \sum_i \left|\frac{\partial W}{\partial \phi_i}\right|^2 \\
&= |(\mu_u + \lambda_S S + \lambda_T T_0) R_d^0 - f\tilde{\nu}_L \tilde{N}^c + \sqrt{2}\lambda_T T_+ R_d^-|^2 \\
&\quad + |(\mu_u + \lambda_S S + \lambda_T T_0) H_u^0 - \sqrt{2}\lambda_T T_- H_u^+|^2 + |\lambda_S H_u^0 R_d^0 + M_R \tilde{N}^c - \lambda_S H_u^+ R_d^-|^2 \\
&\quad + |\lambda_T (H_u^0 R_d^0 + H_u^+ R_d^-)|^2 + |f H_u^0 \tilde{N}^c|^2 + |f H_u^+ \tilde{N}^c|^2 + |f(\tilde{\nu}_L H_u^0 - \tilde{l}_L^- H_u^+) - M_R S|^2 \\
&\quad + |(\mu_u + \lambda_S S - \lambda_T T_0) H_u^+ - \sqrt{2}\lambda_T H_u^0 T_+|^2 + |\sqrt{2}\lambda_T H_u^+ R_d^0|^2 \\
&\quad + |\sqrt{2}\lambda_T H_u^0 R_d^-|^2 + |(\mu_u + \lambda_S S - \lambda_T T_0) R_d^- - f\tilde{l}_L^- \tilde{N}^c + \sqrt{2}\lambda_T T_- R_d^0|^2
\end{aligned} \tag{3.2}$$

and the D-term contribution is given by

$$V_D = \frac{1}{2}\sum_a D^a D^a + \frac{1}{2} D_Y D_Y, \tag{3.3}$$

where

$$D^a = g(H_u^\dagger \tau^a H_u + \tilde{L}_i^\dagger \tau^a \tilde{L}_i + T^\dagger \lambda^a T) + \sqrt{2}(M_2^D T^a + M_2^D T^{a\dagger}). \tag{3.4}$$

The τ^a's are the SU(2) generators in the fundamental representation, whereas λ^a's are the three generators of the SU(2) group in adjoint representation. Again, the D_Y is computed as,

$$D_Y = \frac{g'}{2}(H_u^+ H_u - \tilde{L}_i^+ \tilde{L}_i) + \sqrt{2} M_1^D (S + S^\dagger). \tag{3.5}$$

Here g and g' are $\mathrm{SU}(2)_L$ and $\mathrm{U}(1)_Y$ gauge couplings respectively.

Therefore using eq. (3.4) and eq. (3.5), we expand eq. (3.3) and obtain the contribution to the scalar potential from D-terms as

$$\begin{aligned}
V_D &= \frac{g'^2}{8}(|H_u^+|^2 + |H_u^0|^2 - |\tilde{\nu}_i^0|^2 - |\tilde{l}_i^-|^2)^2 + (M_1^D)^2 (S + S^\dagger)^2 + (M_2^D)^2 (T_0 + T_0^\dagger)^2 \\
&\quad + \frac{g'\sqrt{2}}{2} M_1^D (S + S^\dagger)(|H_u^+|^2 + |H_u^0|^2 - |\tilde{\nu}_i^0|^2 - |\tilde{l}_i^-|^2) \\
&\quad + \frac{g^2}{8}(|H_u^+|^2 - |H_u^0|^2 + |\tilde{\nu}_i^0|^2 - |\tilde{l}_i^-|^2 + 2|T_+|^2 - 2|T_-|^2)^2 \\
&\quad + \frac{g^2}{8}((H_u^+)^* H_u^0 + (\tilde{l}_i^-)^* \tilde{\nu}_i^0 + \sqrt{2}(T_- - T_+) T_0^* + \text{h.c.})^2 - \frac{(M_2^D)^2}{2}((T_+ - T_-) - \text{h.c.})^2 \\
&\quad - \frac{g^2}{8}((H_u^0)^* H_u^+ + (\tilde{l}_i^-)^* \tilde{\nu}_i^0 + \sqrt{2} T_0 (T_+^* + T_-^*) - \text{h.c.})^2 + \frac{(M_2^D)^2}{2}((T_+ + T_-) + \text{h.c.})^2 \\
&\quad + \frac{g M_2^D}{2}((T_+ + T_-) + \text{h.c.})((H_u^+)^* H_u^0 + (\tilde{l}_i^-)^* \tilde{\nu}_i^0 + \sqrt{2}(T_- - T_+) T_0^* + \text{h.c.}) \\
&\quad - \frac{g M_2^D}{2}((T_+ - T_-) - \text{h.c.})((H_u^0)^* H_u^+ + (\tilde{l}_i^-)^* \tilde{\nu}_i^0 + \sqrt{2} T_0 (T_+^* + T_-^*) - \text{h.c.}) \\
&\quad + \frac{\sqrt{2} g M_2^D}{2}(T_0 + h.c.)(|H_u^+|^2 - |H_u^0|^2 + |\tilde{\nu}_i^0|^2 - |\tilde{l}_i^-|^2 + 2|T_+|^2 - 2|T_-|^2).
\end{aligned} \tag{3.6}$$

JHEP01(2014)101

The Soft supersymmetry breaking part of the scalar potential is given by eq. (2.15) and the dominant radiative corrections to the quartic potential are of the form $\frac{1}{2}\delta\lambda_u(|H_u|^2)^2$, $\frac{1}{2}\delta\lambda_\nu(|\tilde{\nu}_a|^2)^2$, and $\frac{1}{2}\delta\lambda_3|H_u^0|^2|\tilde{\nu}_a|^2$. The coefficients of these quartic terms are [45]

$$\begin{aligned}\delta\lambda_u &= \frac{3y_t^4}{16\pi^2}\ln\left(\frac{m_{\tilde{t}_1}m_{\tilde{t}_2}}{m_t^2}\right)+\frac{5\lambda_T^4}{16\pi^2}\ln\left(\frac{m_T^2}{v^2}\right)+\frac{\lambda_S^4}{16\pi^2}\ln\left(\frac{m_S^2}{v^2}\right)\\ &\quad-\frac{1}{16\pi^2}\frac{\lambda_S^2\lambda_T^2}{m_T^2-m_S^2}\left(m_T^2\left\{\ln\left(\frac{m_T^2}{v^2}\right)-1\right\}-m_S^2\left\{\ln\left(\frac{m_S^2}{v^2}\right)-1\right\}\right), \qquad (3.7)\\ \delta\lambda_\nu &= \frac{3y_b^4}{16\pi^2}\ln\left(\frac{m_{\tilde{b}_1}m_{\tilde{b}_2}}{m_b^2}\right)+\frac{5\lambda_T^4}{16\pi^2}\ln\left(\frac{m_T^2}{v^2}\right)+\frac{\lambda_S^4}{16\pi^2}\ln\left(\frac{m_S^2}{v^2}\right)\\ &\quad-\frac{1}{16\pi^2}\frac{\lambda_S^2\lambda_T^2}{m_T^2-m_S^2}\left(m_T^2\left\{\ln\left(\frac{m_T^2}{v^2}\right)-1\}-m_S^2\{\ln\left(\frac{m_S^2}{v^2}\right)-1\right\}\right), \qquad (3.8)\end{aligned}$$

and finally,

$$\begin{aligned}\delta\lambda_3 &= \frac{5\lambda_T^4}{32\pi^2}\ln(\frac{m_T^2}{v^2})+\frac{1}{32\pi^2}\lambda_S^4\ln\left(\frac{m_S^2}{v^2}\right)\\ &\quad+\frac{1}{32\pi^2}\frac{\lambda_S^2\lambda_T^2}{m_T^2-m_S^2}\left(m_T^2\left\{\ln\left(\frac{m_T^2}{v^2}\right)-1\right\}-m_S^2\left\{\ln\left(\frac{m_S^2}{v^2}\right)-1\right\}\right). \qquad (3.9)\end{aligned}$$

These contributions to the Higgs quartic couplings can be very important for the lightest CP-even Higgs boson to have a mass $\sim 125\,\text{GeV}$ for large stop masses and/or large values of the couplings λ_T and λ_S.

3.1 Symmetry breaking and minimization conditions

In minimizing the scalar potential we assume that the neutral scalar fields H_u^0, $\tilde{\nu}_a$ $(a = 1(e))$, S and T acquire real vacuum expectation values v_u, v_a, v_s and v_T, respectively. The scalar fields R_d and $\tilde{N}^c$ carry R-charge 2 and they decouple from the scalar fields mentioned above carrying R-charge 0. In order to write down the minimization conditions, first we split the fields in terms of their real and imaginary parts: $H_u^0 = h_R + ih_I$, $\tilde{\nu} = \tilde{\nu}_R^a + i\tilde{\nu}_I^a$, $S = S_R + iS_I$ and $T = T_R + iT_I$. The resulting minimization equations with respect to h_R, $\tilde{\nu}_R$, T_R, and S_R fields, are

$$\begin{aligned}&(m_{H_u}^2+\mu_u^2)+(b\mu_L^a-fM_Rv_S)(\tan\beta)^{-1}+\lambda_S^2v_S^2+\lambda_T^2v_T^2+2\mu_u\lambda_Sv_S\\ &\quad+2\mu_u\lambda_Tv_T+2\lambda_S\lambda_Tv_Sv_T+f^2v^2\cos^2\beta+\sqrt{2}(g'M_1^Dv_S-gM_2^Dv_T)\\ &\quad+\frac{2\delta\lambda_u+\delta\lambda_3}{2}v^2\cos^2\beta-\frac{(g^2+g'^2+4\delta\lambda_u)}{4}v^2\cos 2\beta=0, \qquad (3.10)\\ &m_{\tilde{L}_a}^2+(b\mu_L^a-fM_Rv_S)\tan\beta+f^2v^2\sin^2\beta+\frac{g^2+g'^2-\delta\lambda_3+2\delta\lambda_\nu}{4}v^2\cos 2\beta\\ &\quad+\left(\frac{\delta\lambda_3+2\delta\lambda_\nu}{4}\right)v^2+\sqrt{2}(gM_2^Dv_T-g'M_1^Dv_S)=0, \qquad (3.11)\end{aligned}$$

$$m_{T_R}^2+\mu_u\lambda_T\frac{v^2}{v_T}\sin^2\beta+\lambda^S\lambda^T\frac{v_S}{v_T}v^2\sin^2\beta+\lambda_T^2v^2\sin^2\beta+\frac{g}{\sqrt{2}}M_2^D\frac{v^2}{v_T}\cos 2\beta = 0, \tag{3.12}$$

$$v_S(m_{S_R}^2+\lambda_S^2v^2\sin^2\beta)+\Big(\mu_u\lambda_Sv^2\sin^2\beta+\lambda_S\lambda_Tv_Tv^2\sin^2\beta+t_S -\frac{g'}{\sqrt{2}}M_1^Dv^2\cos 2\beta-\frac{fM_Rv^2\sin 2\beta}{2}\Big) = 0, \tag{3.13}$$

where we identify $m_{T_R}^2 = m_T^2+b_T+4(M_2^D)^2$, $m_{S_R}^2 = m_S^2+b_S+4(M_1^D)^2+M_R^2$, $\tan\beta = v_u/v_a$ and $v^2 = v_1^2+v_2^2$. The W- and the Z-boson masses can be written as

$$\begin{aligned} m_W^2 &= \frac{1}{2}g^2(v^2+4v_T^2),\\ m_Z^2 &= \frac{1}{2}g^2v^2/\cos^2\theta_W. \end{aligned} \tag{3.14}$$

The tree level ρ-parameter comes out to be

$$\rho\equiv\frac{m_W^2}{m_Z^2\cos^2\theta_W} = 1+\frac{4v_T^2}{v^2}. \tag{3.15}$$

Electroweak precision measurements of the ρ-parameter constrain the triplet vev v_T to be $\lesssim 3\,\text{GeV}$ [46] and can be taken to be zero in the first approximation.

3.2 CP-even neutral scalar sector

With the help of these minimization equations, it is straightforward to write down the neutral CP even scalar squared-mass matrix in the basis $(h_R, \tilde{\nu}_R, S_R, T_R)$. The CP even scalar squared-mass matrix, thus, would be a symmetric 4×4 matrix. Note that we are working in the R-symmetry conserving case.

The elements of the 4×4 CP-even scalar squared-mass matrix M_S^2 are given by

$$\begin{aligned}
(M_S^2)_{11} &= \frac{(g^2+g'^2)}{2}v^2\sin^2\beta+(fM_Rv_S-b\mu_L^a)(\tan\beta)^{-1}+2\delta\lambda_uv^2\sin^2\beta,\\
(M_S^2)_{12} &= f^2v^2\sin 2\beta+b\mu_L^a-\frac{(g^2+g'^2-2\delta\lambda_3)}{4}v^2\sin 2\beta-fM_Rv_S,\\
(M_S^2)_{13} &= 2\lambda_S^2v_Sv\sin\beta+2\mu_u\lambda_Sv\sin\beta+2\lambda_S\lambda_Tvv_T\sin\beta+\sqrt{2}g'M_1^Dv\sin\beta-fM_Rv\cos\beta,\\
(M_S^2)_{14} &= 2\lambda_T^2v_Tv\sin\beta+2\mu_u\lambda_Tv\sin\beta+2\lambda_S\lambda_Tv_Sv\sin\beta-\sqrt{2}gM_2^Dv\sin\beta,\\
(M_S^2)_{22} &= \frac{(g^2+g'^2)}{2}v^2\cos^2\beta+(fM_Rv_S-b\mu_L^a)\tan\beta+2\delta\lambda_\nu v^2\cos^2\beta,\\
(M_S^2)_{23} &= -\sqrt{2}g'M_1^Dv\cos\beta-fM_Rv\sin\beta,\\
(M_S^2)_{24} &= \sqrt{2}gM_2^Dv\cos\beta,\\
(M_S^2)_{33} &= -\mu_u\lambda_S\frac{v^2\sin^2\beta}{v_S}-\frac{\lambda_S\lambda_Tv_Tv^2\sin^2\beta}{v_S}-\frac{t_S}{v_S}+\frac{g'M_1^Dv^2\cos 2\beta}{\sqrt{2}v_S}+\frac{fM_Rv^2\sin 2\beta}{2v_S},
\end{aligned}$$

JHEP01(2014)101

$$
\begin{aligned}
(M_S^2)_{34} &= \lambda_S \lambda_T v^2 \sin^2\beta, \\
(M_S^2)_{44} &= -\mu_u \lambda_T \frac{v^2}{v_T} \sin^2\beta - \lambda_S \lambda_T v_S \frac{v^2}{v_T} \sin^2\beta - \frac{g M_2^D}{\sqrt{2}} \frac{v^2}{v_T} \cos 2\beta.
\end{aligned} \tag{3.16}
$$

Since we want to have the lightest CP-even Higgs boson to be doublet-like and with a mass around 125 GeV, we would require a small vev v_S of the singlet S as well as large radiative corrections to the Higgs boson mass. Because of the choices of R-charges of various fields in this model, one cannot get tree level contributions to the lightest Higgs boson mass proportional to λ_S^2 and λ_T^2 as obtained in [35, 45]. However, there can be an additional contribution to the lightest Higgs boson mass at the tree level proportional to the square of the neutrino Yukawa coupling f and that can be significant when f is $\mathcal{O}(1)$. We shall discuss more on this scenario at a later stage. Note also that the smallness of v_S and v_T can be easily obtained by keeping the corresponding soft supersymmetry breaking mass terms m_S and m_T somewhat larger ($\gtrsim$ a TeV).

3.3 CP-odd neutral scalar sector

In the basis $(h_I, \tilde{\nu}_I, S_I, T_I)$ the elements of the tree-level neutral CP-odd symmetric scalar squared-mass matrix M_P^2 are

$$
\begin{aligned}
(M_P^2)_{11} &= (f M_R v_S - b\mu_L^a)(\tan\beta)^{-1}, \\
(M_P^2)_{12} &= -b\mu_L^a + f M_R v_S, \\
(M_P^2)_{13} &= -f M_R v \cos\beta, \\
(M_P^2)_{14} &= 0, \\
(M_P^2)_{22} &= (f M_R v_S - b\mu_L^a)\tan\beta, \\
(M_P^2)_{23} &= -f M_R v \sin\beta, \\
(M_P^2)_{24} &= 0, \\
(M_P^2)_{33} &= \lambda_S^2 v^2 \sin^2\beta + m_{S_R}^2 - 2b_S - 4(M_1^D)^2, \\
(M_P^2)_{34} &= \lambda_S \lambda_T v^2 \sin^2\beta, \\
(M_P^2)_{44} &= \lambda_T^2 v^2 \sin^2\beta + m_{T_R}^2 - 2b_T - 4(M_2^D)^2.
\end{aligned} \tag{3.17}
$$

The eigenvalues of the CP-odd scalar squared-mass matrix consists of a massless Goldstone boson and three physical CP-odd Higgs bosons. Out of these three physical Higgs bosons, one is essentially the linear combination of h_I and $\tilde{\nu}_I$ whereas the other two eigenstates are composed mainly of S_I and T_I, the imaginary parts of the singlet S and the triplet T.

One can perform the following rotation to separate out the Goldstone mode

$$
\begin{pmatrix} G \\ A \\ S_I' \\ T_I' \end{pmatrix} = \begin{pmatrix} -\sin\beta & \cos\beta & 0 & 0 \\ \cos\beta & \sin\beta & 0 & 0 \\ 0 & 0 & 1 & 0 \\ 0 & 0 & 0 & 1 \end{pmatrix} \begin{pmatrix} h_I \\ \tilde{\nu}_I \\ S_I \\ T_I \end{pmatrix}, \tag{3.18}
$$

where $\tan\beta = v_u/v_a$. The 4×4 squared-mass matrix then reduces to a 3×3 matrix structure from which one can find out the physical CP-odd Higgs bosons.

JHEP01(2014)101

3.4 Charged scalar sector

In this U(1)$_R$ symmetric case the elements of the tree-level charged scalar squared-mass matrix in the basis $(H_u^+, \tilde{L}_a^{-*}, T^+, (T^-)^*)$ are given by $(a = 1(e))$

$$
\begin{aligned}
M_{11}^{\pm 2} &= 2\sqrt{2} g M_2^D v_T - 4 v_S v_T \lambda_S \lambda_T - 4 v_T \lambda_T \mu_u - f^2 v^2 \cos^2\beta + \frac{1}{2} g^2 v^2 \cos^2\beta \\
&\quad + (-b\mu_L^a + f M_R v_S) \cot\beta, \\
M_{12}^{\pm 2} &= -b\mu_L^a + f M_R v_S - \frac{1}{2} f^2 v^2 \sin 2\beta + \frac{1}{4} g^2 v^2 \sin 2\beta, \\
M_{13}^{\pm 2} &= g M_2^D v \sin\beta - \frac{g^2 v v_T \sin\beta}{\sqrt{2}} - \sqrt{2} v \lambda_T (\mu_u + v_S \lambda_S - v_T \lambda_T) \sin\beta, \\
M_{14}^{\pm 2} &= g M_2^D v \sin\beta + \frac{g^2 v v_T \sin\beta}{\sqrt{2}} - \sqrt{2} v \lambda_T (\mu_u + v_S \lambda_S + v_T \lambda_T) \sin\beta, \\
M_{22}^{\pm 2} &= -2\sqrt{2} g M_2^D v_T - f^2 v^2 \sin^2\beta + \frac{1}{2} g^2 v^2 \sin^2\beta + (-b\mu_L^a + f M_R v_S) \tan\beta, \\
M_{23}^{\pm 2} &= g M_2^D v \cos\beta - \frac{g^2 v v_T \cos\beta}{\sqrt{2}}, \\
M_{24}^{\pm 2} &= g M_2^D v \cos\beta + \frac{g^2 v v_T \cos\beta}{\sqrt{2}}, \\
M_{33}^{\pm 2} &= -b_T - 2(M_2^D)^2 + g^2 v_T^2 + \frac{1}{2} g^2 v^2 \cos 2\beta - \frac{g M_2^D v^2 \cos 2\beta}{\sqrt{2} v_T} - \frac{v^2 v_S \lambda_S \lambda_T \sin^2\beta}{v_T} \\
&\quad + v^2 \lambda_T^2 \sin^2\beta - \frac{v^2 \lambda_T \mu_u \sin^2\beta}{v_T}, \\
M_{34}^{\pm 2} &= b_T + 2(M_2^D)^2 - g^2 v_T^2, \\
M_{44}^{\pm 2} &= -b_T - 2(M_2^D)^2 + g^2 v_T^2 - \frac{1}{2} g^2 v^2 \cos 2\beta - \frac{g M_2^D v^2 \cos 2\beta}{\sqrt{2} v_T} - \frac{v^2 v_S \lambda_S \lambda_T \sin^2\beta}{v_T} \\
&\quad - v^2 \lambda_T^2 \sin^2\beta - \frac{v^2 \lambda_T \mu_u \sin^2\beta}{v_T}.
\end{aligned}
\tag{3.19}
$$

In the limit where the vev of the neutral component of the triplet is very small, the triplet essentially decouples from the doublet fields. Considering that, the Goldstone mode can be written as [25, 41],

$$
G^+ = (-\sin\beta H_u^+ + \cos\beta \tilde{L}_a^{-*} + a T^+ + b (T^-)^*), \tag{3.20}
$$

where a and b represents small admixtures of the triplet fields with the doublet Higgs-sneutrino block. In order to evaluate the coefficients a and b, we note that the charged scalar squared-mass matrix follows the eigenvalue equation,

$$
\begin{aligned}
-M_{11}^{\pm 2} \sin\beta + M_{12}^{\pm 2} \cos\beta + M_{13}^{\pm 2} a + M_{14}^{\pm 2} b &= 0, \\
-M_{12}^{\pm 2} \sin\beta + M_{22}^{\pm 2} \cos\beta + M_{23}^{\pm 2} a + M_{24}^{\pm 2} b &= 0.
\end{aligned}
\tag{3.21}
$$

JHEP01(2014)101

Solving for a and b in terms of the charged scalar squared-mass matrix elements, we find $a = b = \frac{\sqrt{2}v_T}{v}$ and finally the expression for the Goldstone mode becomes

$$G^+ = \frac{1}{\sqrt{\rho}}\Big(-\sin\beta H_u^+ + \cos\beta \tilde{L}_a^{-*} + \frac{\sqrt{2}v_T}{v}T^+ + \frac{\sqrt{2}v_T}{v}(T^-)^*\Big), \tag{3.22}$$

where ρ is the appropriate normalization factor and given by $\rho = 1 + \frac{4v_T^2}{v^2}$. The Goldstone boson G^+ gives a mass to W^+ and $G^- \equiv (G^+)^*$ gives a mass to W^-. The other states orthogonal to G^+ are

$$\begin{aligned}
H^+ &= \frac{1}{\sqrt{\rho}}\Big(\cos\beta H_u^+ + \sin\beta \tilde{L}_a^{-*} + \frac{\sqrt{2}v_T}{v}T^+ - \frac{\sqrt{2}v_T}{v}(T^-)^*\Big),\\
T_P^+ &= \frac{1}{\sqrt{\rho}}\Big(\frac{\sqrt{2}v_T}{v}H_u^+ - \frac{\sqrt{2}v_T}{v}\tilde{L}_a^{-*} + \sin\beta T^+ + \cos\beta(T^-)^*\Big),\\
(T_P^-)^* &= \frac{1}{\sqrt{\rho}}\Big(\frac{\sqrt{2}v_T}{v}H_u^+ + \frac{\sqrt{2}v_T}{v}\tilde{L}_a^{-*} - \cos\beta T^+ + \sin\beta(T^-)^*\Big).
\end{aligned} \tag{3.23}$$

Once again we can separate out the Goldstone mode and write down the resulting 3×3 symmetric charged scalar squared-mass matrix in the basis of these orthogonal states (and their charge conjugates) to find out the physical charged scalar states.

3.5 Sum rules

We will conclude the discussion on scalar sector by presenting various sum rules for this model. Let us look at the CP-even neutral scalar squared-mass matrix once again and assume that the singlet and triplet vevs are very small. In such a situation these two fields are effectively decoupled from the theory and as a result the scalar squared-mass matrix becomes, a 2×2 matrix. Under these assumptions, we can write down the elements of the neutral CP-even squared-mass matrix (for the MSSM case see [47]) in a compact form as (see eq. (3.16)),

$$\begin{aligned}
M_{11}^2 &= M_Z^2 \sin^2\beta + \xi\cot\beta,\\
M_{12}^2 &= -\xi + \frac{1}{2}M_Z^2(\alpha - 1)\sin 2\beta = M_{21}^2,\\
M_{22}^2 &= \xi\tan\beta + M_Z^2\cos^2\beta,
\end{aligned} \tag{3.24}$$

where we have defined $\alpha = \frac{2f^2v^2}{M_Z^2}$ and $\xi = fM_R v_S - b\mu_L^a$. Note that we have kept small terms proportional to v_S in this (2×2) light CP-even squared-mass matrix. The eigenvalues of this matrix represent the square of the masses of the two physical doublet-like Higgs bosons (remember that in this model the sneutrino of flavor a plays the role of the down type Higgs) and they are given by

$$\lambda_\pm = \frac{1}{2}\left[(M_Z^2 + \zeta) \pm \Delta\right], \tag{3.25}$$

JHEP01(2014)101

where $\zeta = \frac{2\xi}{\sin 2\beta}$ and

$$\Delta = \left[\left(M_Z^2 - \zeta\right)^2 \cos^2 2\beta + (M_Z^2(1-\alpha) + \zeta)^2 \sin^2 2\beta\right]^{\frac{1}{2}}. \tag{3.26}$$

Similarly, in the decoupling limit of the singlet and triplet fields, the CP odd scalar mass matrix has two eigenvalues. One of which corresponds to the massless Goldstone boson, whereas the other eigenvalue being

$$\zeta = \frac{2(-b\mu_L^a + fM_R v_S)}{\sin 2\beta} \equiv M_A^2. \tag{3.27}$$

The upper bound on the squared-mass of the lightest CP-even Higgs boson ($\lambda_- \equiv m_h^2$) will depend on the value of Δ. With the help of the inequality [41]

$$\left[a^2 \cos^2 2\beta + b^2 \sin^2 2\beta\right]^{\frac{1}{2}} \geqslant \left[a \cos^2 2\beta + b \sin^2 2\beta\right], \tag{3.28}$$

we can write down the tree level upper bound on the lightest CP-even Higgs boson mass depending on whether $\alpha < 1$ or $\alpha > 1$. However, as long as the quantity $\zeta \equiv M_A^2 > M_Z^2$, we find that the tree level upper bound on the lightest CP-even Higgs boson mass is

$$m_h^2 \leqslant \left[M_Z^2 \cos^2 2\beta + f^2 v^2 \sin^2 2\beta\right], \tag{3.29}$$

irrespective of whether $\alpha < 1$ or $\alpha > 1$.

It is very interesting to note that the neutrino Yukawa coupling f provides a tree level correction to the lightest Higgs boson mass. We shall discuss later that in our model f can be as large as $\mathcal{O}(1)$ and in that case this large f would certainly provide a significant correction to the tree level mass of the lightest Higgs boson, requiring very small radiative corrections via the triplet and the singlet as well as from the stop loop.

In a similar way we can obtain a lower bound on the heavy Higgs boson mass irrespective of α for $\zeta \equiv M_A^2 > M_Z^2$ and is given by

$$m_H^2 \geqslant \left[M_Z^2 \sin^2 2\beta + M_A^2 - f^2 v^2 \sin^2 2\beta\right]. \tag{3.30}$$

Finally we also obtain a relation between the trace of the CP-even scalar squared-mass matrix and the trace of the CP-odd scalar squared-mass matrix, which differs from that of the MSSM

$$\mathrm{Tr}(M_S^2) = \mathrm{Tr}(M_P^2) + M_Z^2 + 2(b_S + b_T) + 4\left[(M_1^D)^2 + (M_2^D)^2\right]. \tag{3.31}$$

Looking at the charged Higgs boson squared-mass matrix in the limit of very heavy triplet, we can see that the charged Higgs boson mass ($m_{H^\pm}$) can be written in terms of the CP-odd scalar mass (M_A) and the W boson mass as

$$m_{H^\pm}^2 = M_A^2 + M_W^2 - f^2 v^2 - 4 v_T \lambda_T (\mu_u + \lambda_S v_S). \tag{3.32}$$

Let us also emphasize that we have checked that all the eigenvalues of the CP-even, CP-odd and charged scalar squared-mass matrices (leaving aside the Goldstone bosons) come as positive for a minimum.

JHEP01(2014)101

4 Neutrino sector in R-symmetric case

In the neutral fermion sector we have mixing between the neutralinos, the active neutrino of flavor a, i.e. ν_e and the single right-handed neutrino N^c after the electroweak symmetry breaking.[5] In order to write down the neutral fermion mass matrix, we can separate out the relevant part of the Lagrangian as $\mathcal{L} = (\psi^{0+})^T M_N (\psi^{0-})$, where $\psi^{0+} = (\tilde{b}^0, \tilde{w}^0, \tilde{R}_d^0, N^c)$, with R-charges +1, and $\psi^{0-} = (\tilde{S}, \tilde{T}^0, \tilde{H}_u^0, \nu_e)$, with R- charges -1. The neutral fermion mass matrix M_χ^D is given by

$$M_\chi^D = \begin{pmatrix} M_1^D & 0 & \frac{g' v_u}{\sqrt{2}} & -\frac{g' v_a}{\sqrt{2}} \\ 0 & M_2^D & -\frac{g v_u}{\sqrt{2}} & \frac{g v_a}{\sqrt{2}} \\ \lambda_S v_u & \lambda_T v_u & \mu_u + \lambda_S v_S + \lambda_T v_T & 0 \\ M_R & 0 & -f v_a & -f v_u \end{pmatrix}. \tag{4.1}$$

The mass matrix M_χ^D can be diagonalized by a biunitary transformation involving two unitary matrices V^N and U^N. This will give rise to four Dirac mass eigenstates $\widetilde{\chi}_i^{0+} \equiv \begin{pmatrix} \widetilde{\psi}_i^{0+} \\ \widetilde{\psi}_i^{0-} \end{pmatrix}$, with $i = 1, 2, 3, 4$ and $\widetilde{\psi}_i^{0+} = V_{ij}^N \psi_j^{0+}$, $\widetilde{\psi}_i^{0-} = U_{ij}^N \psi_j^{0-}$. The lightest mass eigenstate $\widetilde{\chi}_4^{0+}$ is identified with the light Dirac neutrino eigenstate. The other two active neutrinos remain massless at the tree level in the R-symmetric limit.

4.1 Dirac mass of the neutrino

As we have mentioned, the smallest eigenvalue of the mass matrix M_χ^D in eq. (4.1) corresponds to the light Dirac neutrino mass. In order to obtain an analytical expression of this small mass, we make a series expansion of $\mathrm{Det}(M_\chi^D - \lambda_s \hat{I})$, with respect to λ_s and then use the characteristic equation to solve for small λ_s [48]

$$\mathrm{Det}(M_\chi^D - \lambda_s \hat{I}) = \mathrm{Det}(M_\chi^D) - \lambda_s \mathrm{Det}(M_\chi^D)\mathrm{Tr}[(M_\chi^D)^{-1}] = 0, \tag{4.2}$$

which implies,

$$\lambda_s = \frac{1}{\mathrm{Tr}[(M_\chi^D)^{-1}]}. \tag{4.3}$$

From eq. (4.3) we obtain the light Dirac neutrino mass as

$$m_{\nu_e}^D = \frac{\left[M_2^D \gamma \tau + v^3 f \sin\beta \omega\right]}{\left[\gamma(\tau + \sqrt{2} M_2^D (M_1^D - f v \sin\beta)) + M_2^D \tau + (v^3 f \sin\beta)(g' \lambda_S - g \lambda_T) - v^2 \sin^2\beta \omega\right]}, \tag{4.4}$$

where,

$$\begin{aligned} \gamma &= (\mu_u + \lambda_S v_S + \lambda_T v_T), \\ \tau &= v \cos\beta (g \tan\theta_W M_R - \sqrt{2} f M_1^D \tan\beta), \\ \omega &= g(M_2^D \lambda_S \tan\theta_W - M_1^D \lambda_T). \end{aligned} \tag{4.5}$$

[5] In the charged fermion sector the charged lepton of flavor a (i.e. $e^\mp$) mixes with the charginos. We shall not discuss it in this work and refer the reader for a thorough discussion in ref. [16].

JHEP01(2014)101

The generic spectrum of this model would include a Dirac neutrino mass ranging from a few hundred eV to few tens of MeV. However by suitably choosing certain relationships involving different parameters, it is possible to have a Dirac neutrino mass within 0.1 eV or so. Therefore, to fit the small neutrino mass, the numerator of eq. (4.4) has to be very small. This can be achieved by assuming $\omega \to 0$ and $\tau \to 0$. In this work we shall analyze the case with $\tau = 0$ and $\omega \to 0$. However, we shall not discuss the other case $\tau \to 0$, $\omega = 0$ in the present work, which can be analyzed in a straightforward way. The choice $\tau = 0$ gives

$$M_R = \frac{\sqrt{2} f M_1^D \tan\beta}{g \tan\theta_W}. \tag{4.6}$$

Thus eq. (4.4) reduces to (neglecting the term containing ω in the denominator)

$$m_{\nu_e}^D = \frac{\left[v^3 f g \sin\beta (M_2^D \lambda_S \tan\theta_W - M_1^D \lambda_T)\right]}{\left[\gamma\sqrt{2} M_2^D (M_1^D - fV\sin\beta) + (v^3 f \sin\beta)(g'\lambda_S - g\lambda_T)\right]}. \tag{4.7}$$

The above expression in eq. (4.7) can be simplified further by assuming $M_1^D \gg fv\sin\beta$ and

$$\lambda_T = \tan\theta_W \lambda_S. \tag{4.8}$$

With all these alterations in place, the neutrino Dirac mass can be expressed in a compact form as

$$m_{\nu_e}^D = \frac{v^3 \sin\beta f g}{\sqrt{2}\gamma M_1^D M_2^D} \lambda_T (M_2^D - M_1^D). \tag{4.9}$$

As mentioned earlier, that in order to have a small neutrino mass, the neutrino Yukawa coupling f need not be very small. By considering a near degeneracy between the bino and wino Dirac masses (M_1^D and M_2^D), it is possible to obtain a small neutrino mass. For example, one can choose $f \sim 10^{-5}$, $\lambda_T \sim 1$, and $(M_2^D - M_1^D) \sim 10^{-2}$ GeV to accommodate a Dirac neutrino mass around 0.1 eV for M_1^D, M_2^D and $\mu_u \sim$ a few hundred GeV. It is pertinent to mention that the requirement of the degeneracy of the Dirac gaugino masses is subject to the relations provided in eqs. (4.6) and (4.8).

However, this near degeneracy between the Dirac gaugino masses can be avoided by assuming $\lambda_T \sim 10^{-4}$, $f \sim 10^{-4}$. As we have discussed previously, the triplet coupling λ_T plays a crucial role to enhance Higgs boson mass via radiative corrections. Therefore, in this case of small λ_T, we have to consider very heavy stops (with masses around a few TeV) for having the lightest CP-even Higgs boson with a mass of 125 GeV. In the other case of $\lambda_T \sim 1$, the stop masses can be around ~ 700 GeV and this makes a phenomenologically interesting scenario. On the other hand, when $f \sim 1$, $\lambda_T \sim 10^{-6}$ and $(M_2^D - M_1^D) \sim 10^{-2}$ GeV, we can still have a light Dirac neutrino mass ~ 0.1 eV and at the same time the lightest Higgs boson mass can be ~ 125 GeV at the tree level without requiring multi-TeV stops or large triplet coupling for substantial radiative corrections. This is a phenomenologically interesting scenario and can be probed further.

Note that we still have two massless active neutrinos in this model and in order to give non-zero masses to these neutrinos one must introduce either additional right-handed

JHEP01(2014)101

neutrino superfields with appropriate Yukawa interactions or look for R-symmetry breaking effects leading to one-loop radiative corrections to neutrino masses. Although the first approach is interesting and should be explored, in the remaining part of our work we shall concentrate on the other approach and introduce a small R-symmetry breaking through a non-zero gravitino mass.

5 R-symmetry breaking

So far we have constrained ourselves in the R-symmetry preserving case. Recent cosmological observations imply a positive but very small vacuum energy or cosmological constant associated with our universe [10]. In the context of a spontaneously broken supergravity theory in a hidden sector [49], having a very small vacuum energy would require a non-zero value of the superpotential in vacuum ($< W >$) and that will break R-symmetry because superpotential carry non-zero R-charges. Since a non-zero gravitino mass also requires a non-zero $< W >$, one can consider the gravitino as the order parameter of the R-symmetry breaking.

The breaking of R-symmetry has to be communicated to the visible sector. In this paper, we shall consider the case of anomaly mediated supersymmetry breaking playing the role of the messenger of R-symmetry breaking as discussed in ref. [15] and coined as anomaly mediated R-symmetry breaking (AMRB). In this situation, apart from the Majorana gaugino masses and the scalar trilinear couplings, all the other R-breaking operators are absent. Finally, since we started with an R-symmetry conserving model and afterwards introduced the breaking of R-symmetry in order to fit neutrino oscillation parameters, it is natural to assume that the R-breaking effects are small. This is the case with small gravitino mass as we shall be discussing later in more detail.

In the AMRB scenario, the majorana gaugino masses, generated due to R-breaking, are related to the gravitino mass in the following way

$$M_i = b_i \frac{g_i^2}{16\pi^2} m_{3/2}, \tag{5.1}$$

where $i = 1, 2, 3$ for bino, wino and gluinos respectively. The coefficients are $b_1 = \frac{33}{5}, b_2 = 1, b_3 = -3$ and one has $g_2 = g$, $g_1 = \sqrt{5/3}g'$. The third generation trilinear scalar couplings are

$$A_t = \frac{\hat{\beta}_{h_t}}{m_t} \frac{m_{3/2}}{16\pi^2} v_u, \quad A_b = \frac{\hat{\beta}_{h_b}}{m_b} \frac{m_{3/2}}{16\pi^2} v_a, \quad A_\tau = \frac{\hat{\beta}_{h_\tau}}{m_\tau} \frac{m_{3/2}}{16\pi^2} v_a, \tag{5.2}$$

where the $\hat{\beta}$'s are written in terms of the usual beta functions as, $\hat{\beta} = \frac{\beta}{16\pi^2}$ and are given by [50, 51],

$$\begin{aligned}
\hat{\beta}_{h_t} &= h_t \left(-\frac{13}{15} g_1^2 - 3g_2^2 - \frac{16}{3} g_3^2 + 6h_t^2 + h_b^2 \right), \\
\hat{\beta}_{h_b} &= h_b \left(-\frac{7}{15} g_1^2 - 3g_2^2 - \frac{16}{3} g_3^2 + h_t^2 + 6h_b^2 + h_\tau^2 \right), \\
\hat{\beta}_{h_\tau} &= h_\tau \left(-\frac{9}{5} g_1^2 - 3g_2^2 + 3h_b^2 + 4h_\tau^2 \right).
\end{aligned} \tag{5.3}$$

JHEP01(2014)101

The trilinear scalar couplings for the first two generations can be obtained in a straightforward way by replacing the Yukawa couplings appropriately.

So, the Lagrangian containing R-breaking effects [15] in the AMRB scenario, can be written as

$$\mathcal{L} = M_1\widetilde{b}^0\widetilde{b}^0 + M_2\widetilde{w}^0\widetilde{w}^0 + M_3\widetilde{g}\widetilde{g} + \sum_{b=2,3} A^l_b \tilde{L}_a \tilde{L}_b \tilde{E}^c_b + \sum_{k=1,2,3} A^d_k \tilde{L}_a \tilde{Q}_k \tilde{D}^c_k \tag{5.4}$$
$$+ \sum_{k=1,2,3} \frac{1}{2} A^{\lambda}_{23k} \tilde{L}_2 \tilde{L}_3 \tilde{E}^c_k + \sum_{j,k=1,2,3;b=2,3} A^{\lambda'}_{bjk} \tilde{L}_b \tilde{Q}_j \tilde{D}^c_k + A^{\nu} H_u \tilde{L}_a \tilde{N}^c + H_u \tilde{Q} A^u \tilde{U}^c.$$

5.1 Neutralino-neutrino mass matrix in R-breaking scenario

Our next task is to incorporate the R-breaking effects in the neutral fermion mass matrix. Because of the presence of Majorana gaugino masses the tree-level neutralino-neutrino mass matrix, written in the basis $(\tilde{b}^0, \tilde{S}, \tilde{w}^0, \tilde{T}, \tilde{R}^0_d, \tilde{H}^0_u, N^c, \nu_e)$, is given by

$$M^M_\chi = \begin{pmatrix} M_1 & M_1^D & 0 & 0 & 0 & \frac{g' v_u}{\sqrt{2}} & 0 & -\frac{g' v_a}{\sqrt{2}} \\ M_1^D & 0 & 0 & 0 & \lambda_S v_u & 0 & M_R & 0 \\ 0 & 0 & M_2 & M_2^D & 0 & -\frac{g v_u}{\sqrt{2}} & 0 & \frac{g v_a}{\sqrt{2}} \\ 0 & 0 & M_2^D & 0 & \lambda_T v_u & 0 & 0 & 0 \\ 0 & \lambda_S v_u & 0 & \lambda_T v_u & 0 & \mu_u + \lambda_S v_S + \lambda_T v_T & 0 & 0 \\ \frac{g' v_u}{\sqrt{2}} & 0 & -\frac{g v_u}{\sqrt{2}} & 0 & \mu_u + \lambda_S v_S + \lambda_T v_T & 0 & -f v_a & 0 \\ 0 & M_R & 0 & 0 & 0 & -f v_a & 0 & -f v_u \\ -\frac{g' v_a}{\sqrt{2}} & 0 & \frac{g v_a}{\sqrt{2}} & 0 & 0 & 0 & -f v_u & 0 \end{pmatrix}. \tag{5.5}$$

In the absence of Majorana gaugino masses ($M_1 = M_2 = 0$), the pure Dirac neutrino case discussed in section 4 is recovered from eq. (5.5) and we have one light Dirac neutrino of mass $m^D_{\nu_e}$. This is equivalent to saying that we have two Majorana neutrinos of mass $-m^D_{\nu_e}$ and $m^D_{\nu_e}$ with opposite CP parities [52].

If the gaugino Majorana mass parameters M_1 and M_2 are non-zero but small compared to the corresponding Dirac gaugino mass parameters M_1^D and M_2^D then the pair of light Majorana neutrinos will be quasi-degenerate and sometimes called a *pseudo-Dirac neutrino*. By increasing the gravitino mass (which means larger M_1 and M_2) one can generate a larger splitting between these two light Majorana neutrino states. Let us discuss these two cases in the context of our model, in detail. Note that in the absence of N^c, the neutralino-neutrino mass matrix cannot produce a non-zero mass of the light neutrino even if the gaugino Majorana mass parameters M_1 and M_2 are non-zero.

5.1.1 Case — 1

In this subsection, we consider a case, where R-breaking effects are very small. The two light mass eigenstates of the neutralino-neutrino matrix in eq. (5.5) are almost degenerate, maximally mixed and they combine to form a (pseudo)Dirac neutrino. We can evaluate the product of these two mass eigenvalues by calculating the ratio of the determinants of the full 8×8 matrix and that of the upper 6×6 block of M^M_χ, without the (N^c, ν_e) sector.

JHEP01(2014)101

Assuming small mixing between this neutrino sector with other neutral fermions we end up with

$$-\lambda^2 = -\left[\frac{v^3 \sin\beta f g}{\sqrt{2}\gamma(M_2^D M_1^D)}\right]^2 \lambda_T^2 \left(M_2^D - M_1^D\right)^2 .$$
$$= -(m_{\nu_e}^D)^2, \tag{5.6}$$

where γ is defined in eq. (4.5) and we have used the relations in eq. (4.6) and eq. (4.8).

5.1.2 Case — 2

Here we are going to consider a relatively lager value of $m_{3/2}$, which is the order parameter for R-breaking. We observe that, with this choice, there is a splitting in masses of the two light Majorana neutrinos with a relatively smaller mixing between the two states. The light neutrinos are predominantly right handed or left handed and the mass eigenstate $N^{c\prime}$ which is mostly a right handed neutrino is heavier than the mass eigenstate ν_e' with a large left handed component. We shall explicitly show this in the section on numerical analysis, but first let us evaluate the lightest Majorana neutrino mass, which corresponds to the mass of ν_e'. This can be done by calculating the ratio of the determinant of the 8×8 neutralino-neutrino mass matrix M_χ^M, to that of the 7×7 upper block of M_χ^M. For a very small neutrino mass we can assume that the eigenvalues of the 7×7 matrix remain unchanged from the seven heavier eigenvalues of the 8×8 matrix. This approximation can be safely implemented as long as $M_1 \gg \frac{g'^2 v_a^2}{2M_1^D}$ and $M_2 \gg \frac{g^2 v_a^2}{2M_2^D}$. We shall choose the mass of the gravitino in such a way that these conditions are satisfied. Therefore the light active Majorana neutrino mass at the tree level, in the R-symmetry breaking scenario is

$$(m_\nu)_{\rm Tree} = -v^2 \frac{\left[g\lambda_T v^2 (M_2^D - M_1^D)\sin\beta\right]^2}{[M_1\alpha^2 + M_2\delta^2]}, \tag{5.7}$$

where

$$\alpha = \frac{2M_1^D M_2^D \gamma \tan\beta}{g\tan\theta_w} + \sqrt{2}v^2\lambda_S \tan\beta(M_1^D \sin^2\beta + M_2^D\cos^2\beta),$$
$$\delta = \sqrt{2}M_1^D v^2 \lambda_T \tan\beta. \tag{5.8}$$

In order to obtain eq. (5.7) we have used once again the relations in eq. (4.6) and eq. (4.8) and γ has been defined previously. We can see from eq. (5.7) that $m_\nu = 0$ (at the tree level) when $M_2^D = M_1^D$ and a small splitting of these Dirac gaugino mass parameters will result in a value of m_ν in the right ballpark provided M_1^D, M_2^D are of the order of a few hundred GeV or 1 TeV with the couplings $\lambda_T, \lambda_S \sim 10^{-4}$ or so. It is very interesting to note that $(m_\nu)_{\rm Tree}$ is independent of the neutrino Yukawa coupling f. This is an artifact of the relation we have used in eq. (4.6) and thus even for a large $f \sim \mathcal{O}(1)$, the tree level Majorana mass of the active neutrino can be kept very small with the above choices of parameters. Our approximate analytical result matches very well with the full numerical analysis as described later in this work.

JHEP01(2014)101

To derive an expression for the mass of the sterile neutrino, we work in the region of parameter space, where the active neutrino becomes a pure left handed neutrino state. Thus by excluding this left handed neutrino state, we are left with a 7×7 neutralino mass matrix and the lightest eigenvalue then would correspond to the mass of the sterile neutrino. In the limit of large M_1^D, together with small couplings[6] λ_S, λ_T, f and considering only the dominant contributions, we eventually obtain the sterile neutrino mass as

$$M_N^R \simeq \left(\frac{M_1}{M_1^D}\right)\left(\frac{M_R}{M_1^D}\right) M_R. \tag{5.9}$$

Substituting the expression of M_R, given in eq. (4.6), we reduce the sterile neutrino mass in the form,

$$M_N^R = M_1 \frac{2f^2 \tan^2\beta}{g'^2}, \tag{5.10}$$

which is independent of M_1^D.

6 eV scale sterile neutrino

The right handed sterile neutrino, introduced in our model can be at the eV scale or at the keV scale depending on the relevant model parameters. In this section we shall analyze the situation when the sterile neutrino is considered to have a mass around 1.2 eV. A mass of the sterile neutrino, in this range, could in principle explain the LSND anomaly. We have discussed in the previous section that there are two different cases, one where the active and sterile neutrinos mix maximally to form a (pseudo)Dirac neutrino, and in the other case there is a relatively large mass splitting between the sterile neutrino and the active neutrino with a very small mixing. In the latter situation there are two distinct Majorana neutrinos in the spectrum. Let us now discuss these two cases separately in the light of the LSND anomaly [38–40].

6.1 Pseudo-Dirac case

When the R-breaking effects are small, the light neutrinos are almost degenerate in mass at the tree level and with near maximal mixing between the two states. In this case, taking into account the possible loop contributions for the active neutrinos as well as the sterile neutrino, the neutrino mass matrix has a two texture zero structure in the basis $(N_R', \nu_e', \nu_\mu, \nu_\tau)$, where the prime signifies that these two states combine to form a (pseudo)Dirac neutrino

$$\begin{pmatrix} \times & \star & 0 & 0 \\ \star & \times & \times & \times \\ 0 & \times & \times & \times \\ 0 & \times & \times & \times \end{pmatrix}. \tag{6.1}$$

[6]This particular choice of the couplings matches with the benchmark points with heavy stops, considered later.

The asterisks in the (12) and (21) elements symbolise the Dirac neutrino mass obtained at tree level from the neutralino-neutrino mass matrix M_χ^M. The crosses in the mass matrix signify the contributions to neutrino masses via loop corrections which we shall discuss elaborately in the next section. The right handed sterile neutrino mixes maximally with the active neutrino in the pseudo-Dirac case. As a result, we took into consideration a small mass of the right handed neutrino, generated by loops. Finally we have a texture two zero structure of the neutrino mass matrix, in the 3+1 scenario.[7]

In order to check whether such a texture of neutrino mass matrix is ruled out or not, we consider a general neutrino mass matrix in the basis $(N_R^{'}, \nu_e^{'}, \nu_\mu, \nu_\tau)$

$$M_\nu = \begin{pmatrix} M_{ss} & M_{se} & M_{s\mu} & M_{s\tau} \\ M_{es} & M_{ee} & M_{e\mu} & M_{e\tau} \\ M_{\mu s} & M_{\mu e} & M_{\mu\mu} & M_{\mu\tau} \\ M_{\tau s} & M_{\tau e} & M_{\tau\mu} & M_{\tau\tau} \end{pmatrix}. \tag{6.2}$$

This mass matrix can be diagonalised by a 4×4 PMNS matrix U which can be constructed with 6 orthogonal rotation matrices. For simplicity, let us consider the scenario with no CP violating phases. The neutrino mass matrix can be obtained from

$$M_\nu = \begin{pmatrix} U_{s1} & U_{s2} & U_{s3} & U_{s4} \\ U_{e1} & U_{e2} & U_{e3} & U_{e4} \\ U_{\mu1} & U_{\mu2} & U_{\mu3} & U_{\mu4} \\ U_{\tau1} & U_{\tau2} & U_{\tau3} & U_{\tau4} \end{pmatrix} \begin{pmatrix} m_1 & 0 & 0 & 0 \\ 0 & m_2 & 0 & 0 \\ 0 & 0 & m_3 & 0 \\ 0 & 0 & 0 & m_4 \end{pmatrix} \begin{pmatrix} U_{s1} & U_{e1} & U_{\mu1} & U_{\tau1} \\ U_{s2} & U_{e2} & U_{\mu2} & U_{\tau2} \\ U_{s3} & U_{e3} & U_{\mu3} & U_{\tau3} \\ U_{s4} & U_{e4} & U_{\mu4} & U_{\tau4} \end{pmatrix}, \tag{6.3}$$

where m_1, m_2, m_3, m_4 are the physical neutrino masses and $m_1 \gg m_2, m_3, m_4$. We compare this with the two texture zero structure given in eq. (6.1)and obtain two equations corresponding to the zeros in the mass matrix. They are as follows

$$\begin{aligned} M_{s\mu} &= m_1 U_{s1} U_{\mu1} + m_2 U_{s2} U_{\mu2} + m_3 U_{s3} U_{\mu3} + m_4 U_{s4} U_{\mu4} = 0, \\ M_{s\tau} &= m_1 U_{s1} U_{\tau1} + m_2 U_{s2} U_{\tau2} + m_3 U_{s3} U_{\tau3} + m_4 U_{s4} U_{\tau4} = 0. \end{aligned} \tag{6.4}$$

These equations can be further simplified with the assumption that the lightest neutrino mass m_4 could be zero. This choice is justified as the oscillation experiments are sensitive to the mass squared differences. With this simplification, eq. (6.4) reduces to

$$\begin{aligned} m_1 U_{s1} U_{\mu1} + m_2 U_{s2} U_{\mu2} + m_3 U_{s3} U_{\mu3} &= 0, \\ m_1 U_{s1} U_{\tau1} + m_2 U_{s2} U_{\tau2} + m_3 U_{s3} U_{\tau3} &= 0. \end{aligned} \tag{6.5}$$

We notice that eq. (6.5) contains $m_1 U_{s1}$, which is much larger than all the other terms. Thus no cancellation between this term and the rest can satisfy eq. (6.5) and we conclude that this texture is not viable to explain LSND anomaly.

[7] A detailed study of two texture zero neutrino mass matrix structure has been performed in [53].

JHEP01(2014)101

6.2 Majorana case

In this section we shall consider a different texture of the light neutrino mass matrix, where we have one Majorana neutrino with a tree level mass $\sim 1.2\,\text{eV}$, but is composed mainly of the right handed sterile neutrino. The other Majorana neutrino has a very small mass at the tree level and it is essentially an active neutrino. Again taking into account possible loop contributions to the active neutrinos, the three texture zero structure[8] of the neutrino mass matrix in the basis $(N'_R, \nu'_e, \nu_\mu, \nu_\tau)$ is given by

$$\begin{pmatrix} \star & 0 & 0 & 0 \\ 0 & \star & \times & \times \\ 0 & \times & \times & \times \\ 0 & \times & \times & \times \end{pmatrix}. \tag{6.6}$$

The asterisks in the (11) and (22) elements represent the tree level Majorana masses of N'_R and ν'_e (with additional loop contribution in the (22) element) whereas all the other masses are generated at the one-loop level. The state N'_R is mostly a right handed sterile neutrino and the active sterile mixing in this case is negligible.

Comparing the neutrino mass matrix obtained in eq. (6.3), with the three texture zero structure of eq. (6.6), we find

$$m_1 U_{s1} U_{i1} + m_2 U_{s2} U_{i2} + m_3 U_{s3} U_{i3} + m_4 U_{s4} U_{i4} = 0 \qquad (i = e, \mu, \tau). \tag{6.7}$$

Again with the assumption of the lightest neutrino mass, $m_4 = 0$, this expression can be simplified further. However, as argued in the previous section, eq. (6.7) cannot be solved by taking into consideration the neutrino oscillation parameters which satisfy the LSND anomaly.

Thus we see that this model as it is, cannot solve the LSND anomaly. Nevertheless, in the next section we shall see that by appropriate choice of parameters we can fit the three flavor global neutrino data in this model and at the same time the sterile neutrino can be accommodated as a keV warm dark matter candidate.

7 Right handed neutrino as a keV warm dark matter

We are considering a situation where the Majorana sterile neutrino acquires a tree level mass of the order of a few keV. We work in a specific region of parameter space, where R-breaking effects are not so large implying that the gravitino mass is around a few GeV ($m_{3/2} \sim 10\,\text{GeV}$). There has been a lot of work on model building aspects of keV sterile neutrino dark matter. For example, keV sterile neutrino dark matter has been discussed in gauge extensions of the SM [56, 57], models of composite Dirac neutrinos [58, 59], 331 models [60, 61], models involving Froggatt-Nielsen mechanism [62] and in several other contexts. A review of different models/mass generation mechanisms can be found in [63]. Various other issues related to keV sterile neutrinos can be found in [64, 65].

[8] A detailed study of three texture zero neutrino mass matrix structure has been performed in [54, 55].

JHEP01(2014)101

Let us give an outline of the case we have considered. The neutrino mass matrix in the basis $(N'_R, \nu'_e, \nu_\mu, \nu_\tau)$ looks like

$$\begin{pmatrix} \star & 0 & 0 & 0 \\ 0 & \star & \times & \times \\ 0 & \times & \times & \times \\ 0 & \times & \times & \times \end{pmatrix}, \tag{7.1}$$

where the stars and crosses have the same meaning as given in eq. (6.6). However, here we have considered a set up in which the sterile neutrino has a mass around a few keV. We also make sure that the active-sterile mixing is very small, and within the valid range given by different X-ray experiments [66–71]. A very rough bound on the active-sterile mixing angle can be written as [72]

$$\theta_{14}^2 \leq 1.8 \times 10^{-5} \left(\frac{1 \text{ keV}}{M_N^R} \right)^5, \tag{7.2}$$

where M_N^R represents the Majorana mass of the right handed sterile neutrino. Therefore, we can treat the right handed neutrino as a decoupled state and work with the effective 3×3 matrix of the active Majorana neutrinos. Note that the (11) element of this 3×3 neutrino mass matrix in the basis $(\nu'_e, \nu_\mu, \nu_\tau)$ receives tree level as well as one-loop level contributions whereas the other entries in this mass matrix comes only through various loop corrections. The size of this tree level contribution to $(m_\nu)_{11}$ is controlled by the model parameters and for suitable choices of the parameters one can obtain a tree level value $(m_\nu)_{\text{Tree}} \lesssim 0.1\,\text{eV}$. Combining with the loop contributions one can then perform a fit to the three flavor global neutrino data.

However, if we wish the keV sterile neutrino to be a candidate for dark matter then it should have the correct relic density ($\Omega_N h^2 \sim 0.1$) and must satisfy the constraints coming from X-ray experiments. An approximate formula for the relic density of sterile neutrinos via the Dodelson-Widrow (DW) [73] mechanism is [66, 73]

$$\Omega_N h^2 \approx 0.3 \left(\frac{\sin^2 2\theta}{10^{-10}} \right) \left(\frac{M_N^R}{100 \text{ keV}} \right)^2, \tag{7.3}$$

where Ω_N is the ratio of density of sterile neutrinos to the total density of the universe and the present value of h is 0.673 [10]. Our numerical scan of the parameter space shows that the correct relic density can be achieved only if $(m_\nu)_{\text{Tree}}$ is extremely small ($\sim 10^{-4}\,\text{eV}$ or so).

Sterile singlet neutrino dark matter can also be produced via the resonant production mechanism [74]. Several other model dependent production mechanisms have been discussed in the literature [63, 75–78]. However, in this work we assume that the relic abundance of keV sterile neutrinos is determined solely by eq. (7.3) resulting from DW mechanism.

There have been different experimental observations which put lower limits on the mass of the keV warm dark matter. For fermionic dark matter particles, a very robust lower bound on their mass comes from Pauli exclusion principle. By demanding that the

JHEP01(2014)101

maximal (Fermi) velocity of the degenerate fermionic gas in the dwarf spheroidal galaxies is less than the escape velocity leads to a lower bound on the mass of the sterile neutrino dark matter $M_N^R > 0.41$ keV [79]. This is the only model independent mass bound which holds for any fermionic dark matter.

Model dependent bounds such as the ones coming from phase space density considerations have put strong lower bounds on the mass of the sterile neutrino acting as a warm dark matter candidate [79–81]. The authors of [82, 83] put a more stringent lower bound on the warm dark matter mass ($M_N^R > 8$–14 keV) by analyzing Lyman-α experimental data. In the context of left-right symmetric model a lower bound of 1.6 keV on the mass of the sterile neutrino warm dark matter has been discussed in [56]. In ref. [57], a lower limit of 0.5 keV on the sterile neutrino dark matter mass has been advocated in low scale left-right theory. In the present work we shall stick to the model independent lower bound of 0.4 keV as discussed above. Moreover, our parameter choices are such that the active sterile neutrino mixing is within the valid range of experimental observations.

In order to get some idea about the numbers involved let us take two examples. With a choice of $M_1^D = 805\,\text{GeV}$, $M_2^D = 800\,\text{GeV}$, the R-symmetry breaking order parameter $m_{3/2} = 5\,\text{GeV}$, $\tan\beta = 5.5$, $\lambda_S = 10^{-4}$, $f = 1.5 \times 10^{-4}$ one produces a tree level mass of the active Majorana neutrino $(m_\nu)_{\text{Tree}} \simeq 2.06 \times 10^{-4}$ eV, and a sterile neutrino of mass around 0.47 keV. The active-sterile mixing is close to 4.35×10^{-7}, which is within the acceptable limit as observed by different X-ray experiments and the relic density of the sterile neutrinos comes out to be $\Omega_N h^2 = 0.117$. Again with another set of parameters such as $M_1^D = 1200.001\,\text{GeV}$, $M_2^D = 1200\,\text{GeV}$, $m_{3/2} = 5\,\text{GeV}$, $\tan\beta = 5$, $\lambda_S = 1.2$ and $f = 1.55 \times 10^{-4}$, we obtain a sterile neutrino of 0.42 keV mass and the tree level active Majorana neutrino mass $(m_\nu)_{\text{Tree}} \simeq 2.2 \times 10^{-4}\,\text{eV}$ with an active-sterile mixing 3.64×10^{-7} and $\Omega_N h^2 = 0.114$.

To conclude this section, we observe that the keV sterile neutrino in this model fits the requirements of a good candidate for warm dark matter. With this note we shall now discuss different loop contributions to the neutrino mass matrix, which provide Majorana masses for the light active neutrinos with appropriate mixing between them.

8 One loop effects to generate neutrino mass

In our model only the electron neutrino acquires a mass at the tree level. The other two neutrinos obtain their masses via one loop diagrams. At one loop level, the neutrino masses are generated from diagrams involving charged lepton-slepton loop, quark-squark loop and neutralino-Higgs loop respectively. We note in passing that similar onle loop calculations have also been performed in [15], which fits neutrino masses via radiative corrections only, without introducing an extra right handed neutrino superfield.

8.1 Charged lepton-slepton loop

We first consider the charged lepton-slepton loop which will generate Majorana mass terms for the neutrinos of all flavors [84]. We consider only the tau-stau loop as other charged lepton-slepton loops have very mild effect as far as neutrino mass is concerned. The con-

JHEP01(2014)101

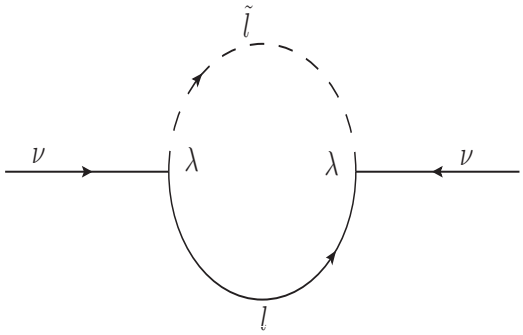

Figure 1. Charged lepton-slepton loop.

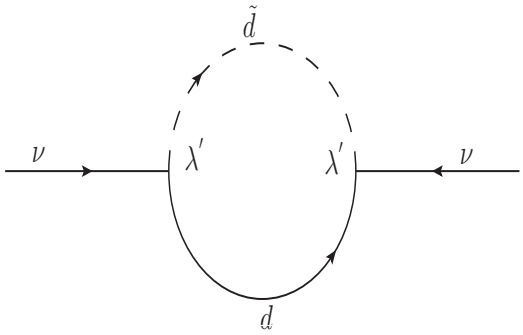

Figure 2. Quark-squark loop for $d = b, s$ quarks and $\tilde{d} = \tilde{b},\ \tilde{s}$ squarks.

tribution of the stau-tau loop (see, figure 1) to the one loop neutrino mass matrix is

$$m_\nu^{l-s} = \frac{1}{(16\pi^2)^2}\left[\frac{m_\tau m_{3/2} v_a}{m_{\tilde{\tau}}^2}\right]\hat{\beta}_\tau \begin{pmatrix} \lambda_{133}^2 & \lambda_{133}\lambda_{233} & 0 \\ \lambda_{233}\lambda_{133} & \lambda_{233}^2 & 0 \\ 0 & 0 & 0 \end{pmatrix} \ln\left(\frac{m_{\tilde{\tau}_1}^2}{m_{\tilde{\tau}_2}^2}\right), \tag{8.1}$$

where we have used the expression of A_τ from eq. (5.2), which provide the necessary lepton number violation of two units in the scalar propagator. Here $m_{\tilde{\tau}_2}^2 > m_{\tilde{\tau}_1}^2$ represent the physical squared-masses of the staus and $m_{\tilde{\tau}}^2 \simeq m_{\tilde{\tau}_2}^2$. In the above mass matrix we considered $e = 1$, and $\mu, \tau = 2, 3$ respectively, keeping in mind that λ is antisymmetric in the first two indices. Because of this antisymmetry property of the coupling λ, some of the elements in m_ν^{l-s} are zero.

8.2 Squark-quark loop

The squark-quark loop will also contribute to the light neutrino Majorana mass matrix [84]. Here we have taken into account bottom and strange squark-quark loop as shown in figure 2.

JHEP01(2014)101

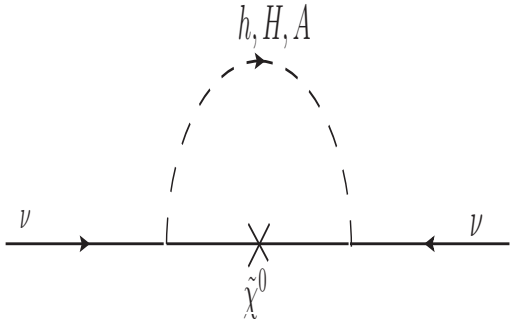

Figure 3. Neutralino-Higgs boson loop.

The contribution of quark-squark loop to the one loop neutrino mass matrix is

$$
\begin{aligned}
m_\nu^{q-s} = & \frac{3}{(16\pi^2)^2}\left[\frac{m_{3/2}v_a}{m_{\tilde{b}}^2}\right]\hat{\beta}_b \\
& \times\left[m_b\begin{pmatrix}\lambda'^2_{133} & \lambda'_{133}\lambda'_{233} & \lambda'_{133}\lambda'_{333}\\ \lambda'_{133}\lambda'_{233} & \lambda'^2_{233} & \lambda'_{233}\lambda'_{333}\\ \lambda'_{333}\lambda'_{133} & \lambda'_{333}\lambda'_{233} & \lambda'^2_{333}\end{pmatrix}\ln\left(\frac{m^2_{\tilde{b}_1}}{m^2_{\tilde{b}_2}}\right)+m_s\begin{pmatrix}0 & 0 & 0\\ 0 & \lambda'_{223}\lambda'_{232} & \lambda'_{223}\lambda'_{332}\\ 0 & \lambda'_{323}\lambda'_{232} & \lambda'_{323}\lambda'_{332}\end{pmatrix}\ln\left(\frac{m^2_{\tilde{b}_1}}{m^2_{\tilde{b}_2}}\right)\right] \\
& +\frac{3}{(16\pi^2)^2}\left[\frac{m_{3/2}v_a}{m_{\tilde{s}}^2}\right]\hat{\beta}_s \\
& \times\left[m_b\begin{pmatrix}0 & 0 & 0\\ 0 & \lambda'_{232}\lambda'_{223} & \lambda'_{232}\lambda'_{323}\\ 0 & \lambda'_{332}\lambda'_{223} & \lambda'_{332}\lambda'_{323}\end{pmatrix}\ln\left[\frac{m^2_{\tilde{s}_1}}{m^2_{\tilde{s}_2}}\right]+m_s\begin{pmatrix}\lambda'^2_{122} & \lambda'_{122}\lambda'_{222} & \lambda'_{122}\lambda'_{322}\\ \lambda'_{122}\lambda'_{222} & \lambda'^2_{222} & \lambda'_{222}\lambda'_{322}\\ \lambda'_{322}\lambda'_{122} & \lambda'_{322}\lambda'_{222} & \lambda'^2_{322}\end{pmatrix}\ln\left[\frac{m^2_{\tilde{s}_1}}{m^2_{\tilde{s}_2}}\right]\right].
\end{aligned}
\tag{8.2}
$$

$m^2_{\tilde{b}_1,\tilde{b}_2}$ $m^2_{\tilde{s}_1,\tilde{s}_2}$ are the physical squared-masses of the sbottom squarks and strange squarks respectively with $m^2_{\tilde{b}_2} > m^2_{\tilde{b}_1}$, $m^2_{\tilde{s}_2} > m^2_{\tilde{s}_1}$ and $m^2_{\tilde{b}} \simeq m^2_{\tilde{b}_2}$, $m^2_{\tilde{s}} \simeq m^2_{\tilde{s}_2}$. Since $\hat{\beta}_b \gg \hat{\beta}_s$ and $m_b \gg m_s$, the dominant contribution to the neutrino mass matrix arises from the first two terms in eq. (8.2) as long as we assume $m^2_{\tilde{s}} \gg m^2_{\tilde{b}}$. The other terms have a sub dominant contribution to the neutrino masses and therefore, it is safe to consider only the first two terms for computing the neutrino mass eigenvalues.

8.3 Neutralino-Higgs boson loop

We now consider the loop consisting of neutralino and Higgs propagators to generate Majorana mass of neutrinos [85, 86]. This is shown in figure 3. The loop contribution is proportional to the Majorana gaugino mass parameters M_1 and M_2, which are much smaller than the mass of the corresponding physical neutralino states. Note that the bilinear term $b\mu_L H_u^0\tilde{\nu}^a$ in the scalar potential can be large in this model and this loop contribution can be significant. In order to compute this loop we consider a simplified scenario where the singlet and the triplet states are integrated out and we are therefore left only with the H_u and $\tilde{\nu}^a$ fields as considered earlier in the discussion of the scalar sector, generating the CP-even physical states h, H and the CP-odd state A.

JHEP01(2014)101

Majorana mass term of a neutrino implies lepton number violation by two units. This is provided by the Majorana mass insertion in the neutralino propagator. The contribution to the neutrino mass matrix from this loop is given by

$$
\begin{aligned}
(m_\nu)_{11} = & \frac{g^2}{64\pi^2} \sum_{\gamma=1,2} \left[Z_{\gamma 2} - \tan\theta_W Z_{\gamma 1}\right]^2 \frac{M_1}{2} \\
& \left[\cos^2\alpha B_0(0, m_H^2, m_{\tilde{\chi}^0}^2) + \sin^2\alpha B_0(0, m_h^2, m_{\tilde{\chi}^0}^2) - \sin^2\beta B_0(0, m_A^2, m_{\tilde{\chi}^0}^2)\right] \\
& + \frac{g^2}{64\pi^2} \sum_{\gamma=3,4} \left[Z_{\gamma 2} - \tan\theta_W Z_{\gamma 1}\right]^2 \frac{M_2}{2} \\
& \left[\cos^2\alpha B_0(0, m_H^2, m_{\tilde{\chi}^0}^2) + \sin^2\alpha B_0(0, m_h^2, m_{\tilde{\chi}^0}^2) - \sin^2\beta B_0(0, m_A^2, m_{\tilde{\chi}^0}^2)\right],
\end{aligned}
\tag{8.3}
$$

where $\tan\beta = v_u/v_a$ and we have used

$$
\begin{aligned}
\tilde{\nu}_R^a &\simeq v_1 + \frac{1}{\sqrt{2}}\big(H\cos\alpha - h\sin\alpha\big), \qquad (a = 1(e)) \\
h_R &\simeq v_2 + \frac{1}{\sqrt{2}}\big(H\sin\alpha + h\cos\alpha\big), \\
\tilde{\nu}_I^a &\simeq \frac{1}{\sqrt{2}}(G\cos\beta + A\sin\beta).
\end{aligned}
\tag{8.4}
$$

The summation in eq. (8.3) is taken over two pairs of nearly degenerate pseudo-Dirac heavier neutralino states $m_{\tilde{\chi}_{1,2}}$ and $m_{\tilde{\chi}_{3,4}}$, which are predominantly bino ($\tilde{b}^0$) and wino ($\tilde{w}^0$) respectively. Here we have assumed that $|m_{\tilde{\chi}_{1,2}}| \simeq M_1^D \pm \frac{M_1}{2}$ and $|m_{\tilde{\chi}_{3,4}}| \simeq M_2^D \pm \frac{M_2}{2}$ and for a given pair the neutralino mixing matrix elements $Z_{\gamma 2}$ and $Z_{\gamma 1}$ does not change for $\gamma = (1,2)$ and $(3,4)$. B_0 is a Passarino-Veltman function and follow its definition as mentioned in [84–86]. It is important to note that this one loop contribution adds only to the (11) element of the effective 3×3 neutrino mass matrix. The other neutrino flavors do not get any contribution to their masses from this loop because the corresponding sneutrinos do not mix with H_u.

9 Numerical analysis

We now present the results of our detailed numerical investigations to fit the lightest Higgs boson mass, neutrino masses and mixing angles as well as the keV sterile neutrino mass and its mixing with the active neutrino. As mentioned earlier in the text, we analyze two situations, one with small singlet and triplet couplings (λ_S and λ_T respectively), which would imply heavy stops to fit the lightest Higgs boson mass whereas the other case with light stop mass requires large λ_S and λ_T, which would provide significant radiative corrections to the lightest Higgs boson mass. A set of benchmark points for the latter case is provided below in table 2.

We chose a relatively larger value of the Dirac wino mass consistent with the allowed range of $\tan\beta$ ($2.7 \leq \tan\beta \leq 17.4$) obtained from the deviation in the couplings of the

JHEP01(2014)101

Parameters	BP-1	BP-2	BP-3
M_1^D	1200.001 GeV	1000.001 GeV	800.001 GeV
M_2^D	1200 GeV	1000 GeV	800 GeV
$\tan\beta$	5	7	10
λ_S	1.25	1.1	0.98
λ_T	$\lambda_S \tan\theta_W \sim 0.69$	0.6	0.54
μ	590 GeV	530 GeV	650 GeV
t_S	$(200)^3$ $(\text{GeV})^3$	$(200)^3$ $(\text{GeV})^3$	$(200)^3$ $(\text{GeV})^3$
$b\mu_L$	$-(200)^2$ $(\text{GeV})^2$	$-(200)^2$ $(\text{GeV})^2$	$-(200)^2$ $(\text{GeV})^2$
m_S	7.6 TeV	10 TeV	18 TeV
m_T	5.46 TeV	5.8 TeV	1.9 TeV
v_S	-0.6 GeV	-0.3 GeV	-0.1 GeV
v_T	0.1 GeV	0.1 GeV	0.05 GeV
f	1.55×10^{-4}	1.1×10^{-4}	1.0×10^{-4}
M_R	3.67 GeV	3 GeV	3.16 GeV
$m_{\tilde{t}_1} = m_{\tilde{t}_2}$	600 GeV	900 GeV	1.2 TeV
b_S	1 TeV	1 TeV	1 TeV
b_T	1 TeV	1 TeV	1 TeV
$m_{3/2}$	5 GeV	6 GeV	3 GeV
m_h	125.15 GeV	124.9 GeV	123.7 GeV
M_N^R	0.42 keV	0.51 keV	0.43 keV
$(m_\nu)_{\text{Tree}}$	2.17×10^{-4} eV	1.86×10^{-4} eV	2.4×10^{-4} eV
θ_{14}^2	5.05×10^{-7}	3.64×10^{-7}	5.53×10^{-7}
$\Omega_N h^2$	0.1121	0.114	0.122

Table 2. Benchmark points (with large λ_S and λ_T) to calculate the lightest Higgs boson mass, light active neutrino mass, mass of the sterile neutrino as well as its mixing with active neutrino and the relic density of sterile neutrino dark matter.

Z boson to charged leptons as well as from the τ Yukawa couplings [16]. In order to fit the neutrino data, we choose the Dirac bino mass very close to the Dirac wino mass. Let us emphasize that in this model a large Dirac gaugino mass does not introduce any logarithmically divergent contribution to scalar masses squared because it is cancelled by the new scalar loop contributions [34].

In table 3 we show benchmark points corresponding to small $\lambda_T \sim 10^{-4}$. In this case, in order to fit the neutrino data, one does not require a strong degeneracy between M_1^D and M_2^D. It is worth mentioning once again that we have reduced the number of independent parameter of the model by assuming certain relations between some of them as shown in eqs. (4.6) and (4.8). One can observe from these two tables that the benchmark points provide a lightest Higgs boson mass around 125 GeV, a sterile neutrino mass in the keV range along with a very small active-sterile mixing and a very small tree level active neutrino Majorana mass. The mass and mixing of the sterile neutrino are in the allowed range of values coming from X-ray observations and it can be accommodated as a warm dark matter candidate in our model.

JHEP01(2014)101

Parameters	BP-4	BP-5	BP-6
M_1^D	1018 GeV	805 GeV	604 GeV
M_2^D	1000 GeV	800 GeV	600 GeV
$\tan\beta$	10	5.5	7
λ_S	10^{-4}	10^{-4}	10^{-4}
λ_T	$\lambda_S \tan\theta_W \sim 5.5 \times 10^{-5}$	5.5×10^{-5}	5.5×10^{-5}
μ	700 GeV	500 GeV	580 GeV
t_S	$(200)^3$ $(\text{GeV})^3$	$(200)^3$ $(\text{GeV})^3$	$(200)^3$ $(\text{GeV})^3$
$\text{b}\mu_L$	$-(200)^2$ $(\text{GeV})^2$	$-(200)^2$ $(\text{GeV})^2$	$-(200)^2$ $(\text{GeV})^2$
m_S	12 TeV	11.6 TeV	11 TeV
m_T	11 TeV	10.14 TeV	9 TeV
v_S	-0.1 GeV	-0.1 GeV	-0.1 GeV
v_T	0.1 GeV	0.1 GeV	0.1 GeV
f	0.92×10^{-4}	1.5×10^{-4}	1.2×10^{-4}
M_R	3.69 GeV	2.62 GeV	2 GeV
$m_{\tilde{t}_1} = m_{\tilde{t}_2}$	6.5 TeV	6.5 TeV	6.5 TeV
b_S	1 TeV	1 TeV	1 TeV
b_T	1 TeV	1 TeV	1 TeV
$m_{3/2}$	3.5 GeV	5 GeV	6 GeV
m_h	126 GeV	123.1 GeV	124.9 GeV
M_N^R	0.41 keV	0.47 keV	0.59 keV
$(m_\nu)_{\text{Tree}}$	2.41×10^{-4} eV	2.06×10^{-4}eV	1.6×10^{-4} eV
θ_{14}^2	5.85×10^{-7}	4.35×10^{-7}	2.7×10^{-7}
$\Omega_N h^2$	0.119	0.117	0.114

Table 3. Benchmark points with small λ_S and λ_T.

In figure 4(a) the contours of the tree level mass $(m_\nu)_{\text{Tree}}$ of the light active neutrino in the (M_1^D-M_2^D) plane exhibits the degeneracy required for these two parameters in order to have a small neutrino mass. Figure 4(b) shows that the active-sterile mixing is also dependent on the degeneracy of M_1^D and M_2^D. Since the X-ray experiments provide very stringent constraints on the mixing, one is compelled to choose the Dirac gaugino masses close to each other. For these two plots, all the other parameters are fixed at the values of BP-4. In figure 4(c) we show the variation of the sterile neutrino mass in the (f-$m_{3/2}$) plane. The figure shows that for a fixed f, a larger gravitino mass produces a larger mass of the sterile neutrino. Again we expect this to happen because the gravitino is the order parameter of R-breaking and therefore, a larger gravitino mass creates a larger mass splitting between the sterile and the active neutrino, which would be zero in the absence of gravitino mass. This way the sterile neutrino mass gets more enhanced whereas the active neutrino mass becomes smaller. On the contrary the active-sterile mixing decreases with $m_{3/2}$ for a fixed f as shown in figure 4(d). This is also expected, as a larger gravitino mass increases the mass of the sterile neutrino and thus reduces its mixing with the active neutrino. In figures 4 (c) and 4(d), we have fixed M_2^D at 1 TeV and M_1^D at 1.018 TeV,

JHEP01(2014)101

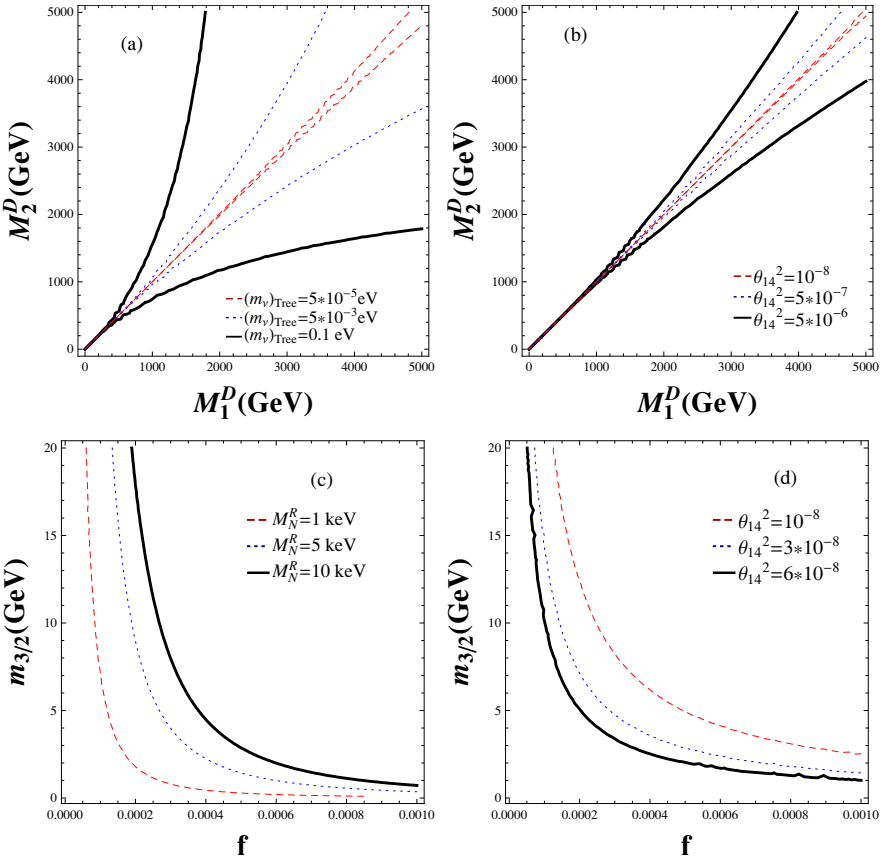

Figure 4. Figure (a) represents contours of tree level light neutrino mass $(m_\nu)_{\rm Tree}$ in the (M_1^D–M_2^D) plane. The black thick line represents $(m_\nu)_{\rm Tree} = 0.1\,{\rm eV}$. The blue dotted line and the red dashed line represent $(m_\nu)_{\rm Tree} = 5\times10^{-3}\,{\rm eV}$ and $5\times10^{-5}\,{\rm eV}$, respectively. Figure (b) represents active-sterile mixing (θ_{14}^2) in the same (M_1^D–M_2^D) plane. The black thick line represents the contour of 5×10^{-6} and the blue dotted line and the red dashed line represent contours of 5×10^{-7} and 10^{-8}, respectively. Figures (c) and (d) show the contours of sterile neutrino mass (M_N^R) and θ_{14}^2 in the (f–$m_{3/2}$) plane. In figure (c) the black thick line corresponds to $M_N^R = 10$ keV whereas the blue dotted line and the red dashed line show contours of $M_N^R = 5$ keV and 1 keV, respectively. In figure (d) the black thick line shows a mixing of 6×10^{-8} and the blue and the red line show $\theta_{14}^2 = 3\times10^{-8}$ and 10^{-8}, respectively.

corresponding to BP-4 in table 3. In figure 5 the contours of (a) M_N^R, (b) θ_{14}^2 and (c) $(m_\nu)_{\rm Tree}$ are shown in the (M_1^D–$m_{3/2}$) plane and in (d) contours of θ_{14}^2 are presented in the (f–M_1^D) plane for other parameter choices shown in BP-4. One can see from figure 5(a) that for large values of M_1^D, the sterile neutrino mass M_N^R is almost insensitive to M_1^D as expected from eq. (5.10). However, the mixing θ_{14}^2 increases with M_1^D for a fixed $m_{3/2}$ and this is because of the fact that the light neutrino mass m_ν also increases with M_1^D for a fixed M_2^D and $m_{3/2}$ (see figure 5(c)) and thus leads to an increase in θ_{14}^2. The variation of θ_{14}^2 in the (f–M_1^D) plane can also be explained in a similar way by looking at eq. (5.7).

We have also presented two scatter plots in the (M_N^R-θ_{14}^2) plane in figures 6 and 7 showing the allowed region after taking into account the constraints from the X-ray experiments as well as the lower bound of 0.4 keV on the sterile neutrino mass, discussed earlier. On

JHEP01(2014)101

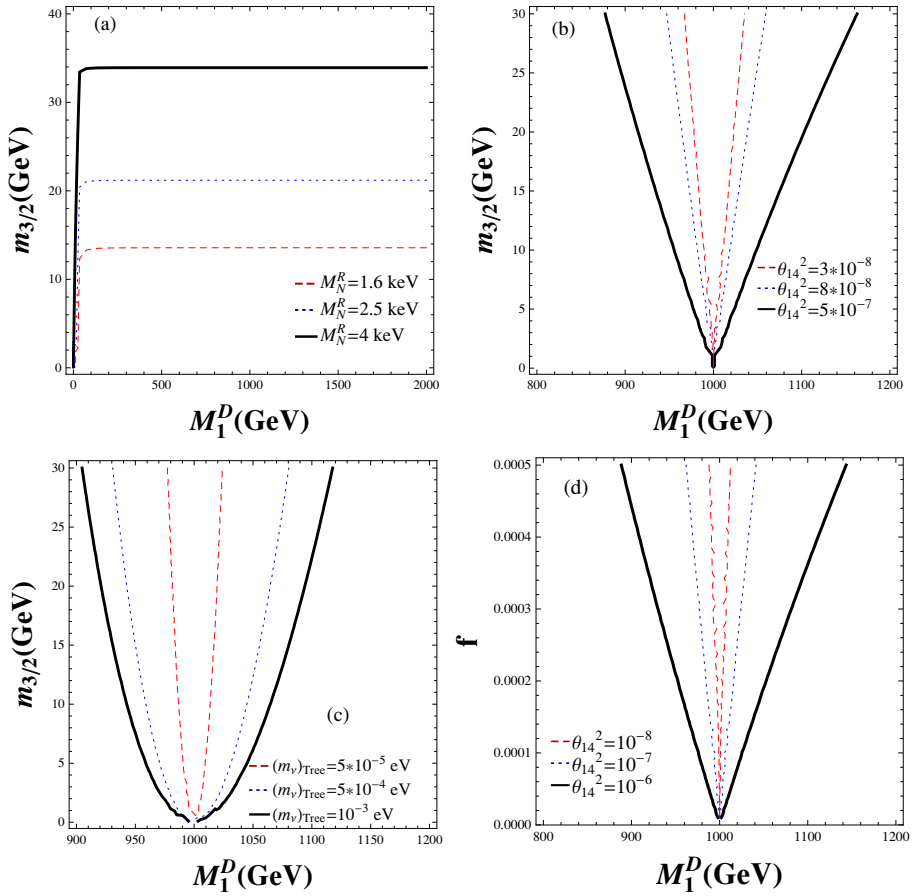

Figure 5. Figure (a) represents contours of M_N^R in the (M_1^D–$m_{3/2}$) plane. The red dashed line shows a sterile neutrino of mass 1.6 keV whereas the blue dotted and the thick black line shows a sterile neutrino mass of 2.5 keV and 4 keV, respectively. In figure (b) θ_{14}^2 contours are shown in the same plane. The contours are 5×10^{-7} (black-thick), 8×10^{-8} (blue-dotted) and 3×10^{-8} (red-dashed), respectively. In figure (c) we show the variation of tree level active neutrino mass m_ν in the (M_1^D–$m_{3/2}$). The outermost contours represent $(m_\nu)_{\rm Tree} = 10^{-3}\,$eV. Finally in figure (d) we plot the contours of θ_{14}^2 in the (M_1^D–f) plane.

top of that we have also shown the points satisfying the correct dark matter relic density at 3σ ($\Omega_{\rm DM}h^2 = 0.1199 \pm 0.0027$ at 1σ) as obtained from the recent observations of the PLANCK experiment [10].

Note that in this model the gravitino is the LSP for the parameter region discussed so far and can, in principle, be a candidate for dark matter. So, in general, one can have two component dark matter in this model. However, in figures 6 and 7 we have assumed that the dark matter relic density is entirely due to the sterile neutrino. A more detailed analysis of this two component dark matter scenario is beyond the scope of the present work. In order to generate these two plots we have varied all the parameters, which play an important role in sterile neutrino mass and active sterile mixing. This plot has been generated by varying the model parameters in the following range: $800\,\text{GeV} \leq M_1^D,\ M_2^D \leq 850\,\text{GeV}$, $1\,\text{GeV} \leq m_{3/2} \leq 40$ GeV, $10^{-5} \leq f \leq 8 \times 10^{-4}$ and $2.7 \leq \tan\beta \leq 17$. We have

JHEP01(2014)101

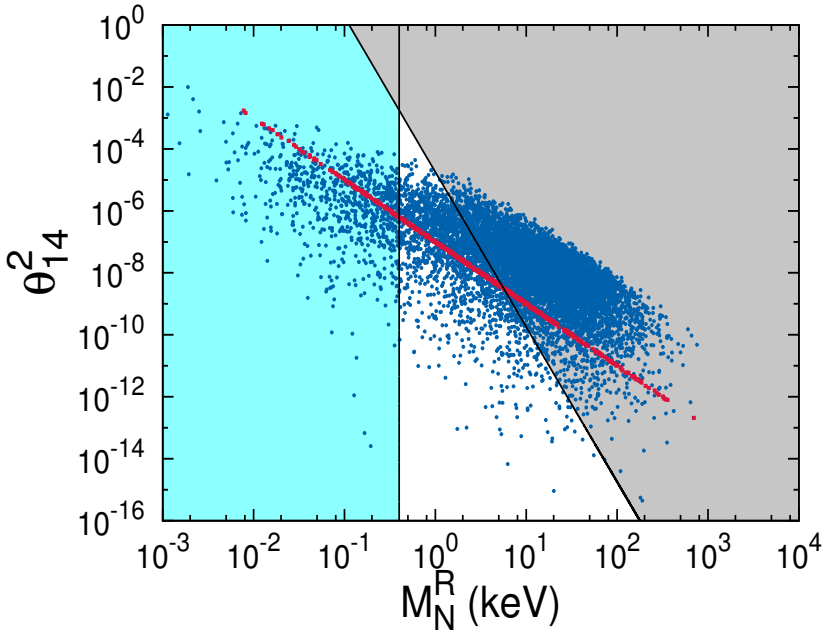

Figure 6. Scatter plot in sterile neutrino mass and active-sterile mixing plane showing the allowed regions, in the heavy stop scenario. The grey region shows the part of the parameter space excluded by the X-ray experiments. Lower bound on sterile neutrino mass excludes the blue region to the left of the vertical line and the thick red band represents the parameter points which satisfy correct dark matter relic density, at 3σ.

kept $\lambda_S \sim 10^{-4}$ and so obviously these points represent the heavy stop scenario. The grey region is disallowed by the constraints from X-ray observations whereas the red line at 0.4 keV and the blue region to its left is ruled out by the lower bound on sterile neutrino mass. Finally, note that by varying the stop mass we ensured that all the scattered points in this plot produced the lightest Higgs boson mass in the range $(123 - 127)$ GeV. In figure 7, we show the results of our parameter space scan in the light stop scenario. In this plot we have used $\lambda_S \sim$ 1.1 and $1\,\text{GeV} \leq m_{3/2} \leq 40\,\text{GeV}$ whereas f and $\tan\beta$ are varied in the same range as before.

We discussed earlier that for large λ_S, the Dirac gaugino masses M_1^D and M_2^D need to be almost degenerate in order to fit a small tree level mass of the active neutrino. Therefore in this plot we fixed $M_1^D = 1000.001\,\text{GeV}$ and $M_2^D = 1000\,\text{GeV}$. The grey and the blue regions again represent the parameter points ruled out by X-ray experiments and lower limit on the sterile neutrino mass respectively. We have also ensured that each and every point in this scattered plot produce a Higgs boson mass in the range $(123 - 127)$ GeV. In figure 8 we showed the variation of the relic density of the sterile neutrino with its mass. The blue scattered points respect the X-ray constraints and the Higgs boson mass within the range $(123 - 127)$ GeV. The grey region shows the parameter space disfavored by the Pauli exclusion principle discussed earlier. The red-circle, green-triangle and orange-square points represent tree level neutrino mass greater than $10^{-5}, 10^{-4}$ and 10^{-3} eV respectively. We observe that in order to have a sterile neutrino as a warm dark matter candidate in our model, the neutrino mass at the tree level has to be very small.

JHEP01(2014)101

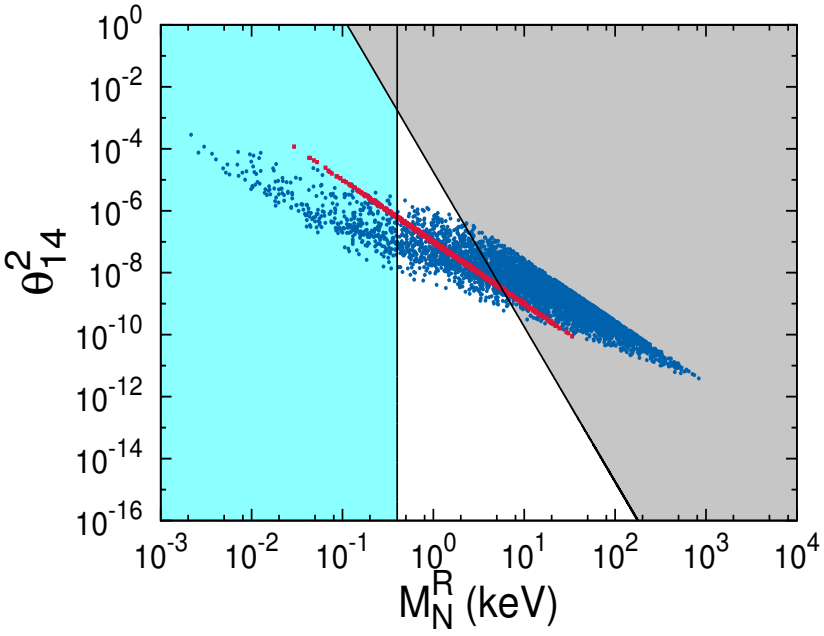

Figure 7. Scatter plot in the (M_N^R–θ_{14}^2) plane showing the allowed regions, in the light stop scenario. The colored(shaded) regions are the same as described in figure 6.

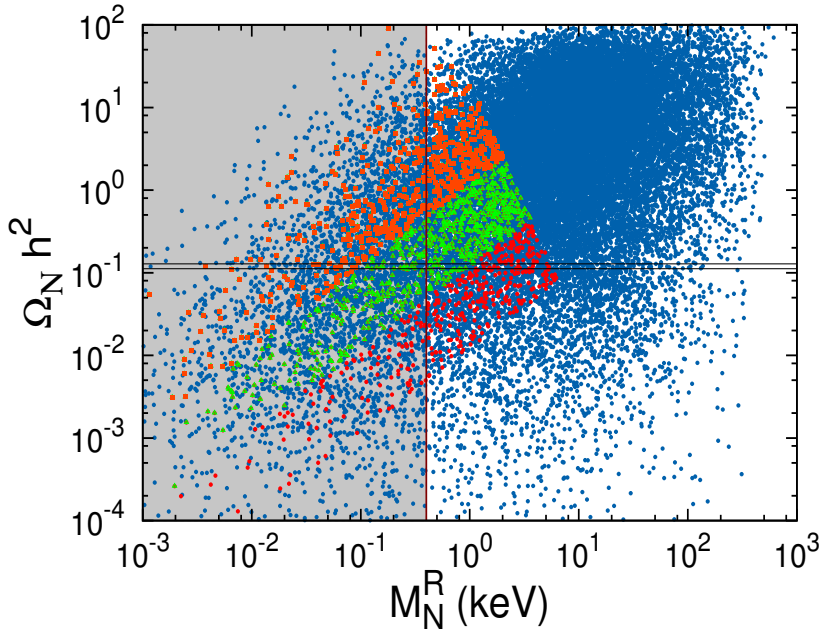

Figure 8. Scatter plot in the (M_N^R–$\Omega_N h^2$) plane showing the allowed regions, in the heavy stop scenario. The grey region describes the lower bound of the sterile neutrino mass, for it to become a warm dark matter candidate. All the scattered points satisfy the X-ray constraints. The red-circle scattered points show $(m_\nu)_{\mathrm{T}ree} > 10^{-5}$eV. The green(triangle) and the orange(square) points represent $(m_\nu)_{\mathrm{T}ree} > 10^{-4}, 10^{-3}$ respectively. The horizontal band is the 3σ allowed region for the dark matter relic abundance.

JHEP01(2014)101

9.1 Neutrino masses and mixing: inverted hierarchy

For inverted hierarchy the best-fit values of solar and the atmospheric neutrino mass squared differences and the three mixing angles are as follows [5] $\Delta m^2_{21} = 7.62 \times 10^{-5}\text{eV}^2$, $|\Delta m^2_{31}| = 2.43 \times 10^{-3}\text{eV}^2$, $\theta_{12} = 34.4^\circ$, $\theta_{23} = 50.8^\circ$ and $\theta_{13} = 9.1^\circ$, where $\Delta m^2_{ij} \equiv m^2_i - m^2_j$. The neutrino mass matrix can be obtained using

$$m_\nu = U_{PMNS} \begin{pmatrix} m_1 & 0 & 0 \\ 0 & m_2 & 0 \\ 0 & 0 & m_3 \end{pmatrix} U^T_{PMNS}, \tag{9.1}$$

where the standard PMNS matrix U_{PMNS}, with vanishing CP violating phases is of the form

$$U_{\text{PMNS}} = \begin{pmatrix} c_{12}c_{13} & s_{12}c_{13} & s_{13} \\ -s_{12}c_{23} - c_{12}s_{23}s_{13} & c_{12}c_{23} - s_{12}s_{23}s_{13} & s_{23}c_{13} \\ s_{12}s_{23} - c_{12}c_{23}s_{13} & -c_{12}s_{23} - s_{12}c_{23}s_{13} & c_{23}c_{13} \end{pmatrix}, \tag{9.2}$$

and m_1, m_2 and m_3 are the neutrino mass eigenvalues. Since the oscillation experiments are sensitive only to the mass squared differences, therefore for simplicity, we can assume the lightest neutrino mass m_3 to be zero in this case. Thus we have $m^2_1 = |\Delta m^2_{31}|$ and $m^2_2 = \Delta m^2_{21} + m^2_1$. For example, using the central values of the oscillation parameters mentioned above, the three flavor neutrino mass matrix in the inverted hierarchy case comes out to be

$$m^{IH}_\nu = \begin{pmatrix} 0.049 & -0.0059 & -0.0052 \\ -0.0059 & 0.0211 & -0.024 \\ -0.0052 & -0.024 & 0.0311 \end{pmatrix}. \tag{9.3}$$

The three flavor active neutrino mass matrix in our model is composed mainly of the one-loop radiative corrections as discussed above because the tree level contribution to $(m_\nu)_{11}$ is very small in order to have the correct relic density of the keV sterile neutrino dark matter. We shall now present the results of our numerical analysis in order to fit the three-flavor global neutrino data in our model in the inverted hierarchy scenario. We shall confine ourselves in the parameter region which will produce the correct value for the lightest Higgs boson mass and where the sterile right handed neutrino can be a good candidate for keV warm dark matter.

Note that there are contributions from the tau-stau, quark-sqaurk and neutralino-Higgs loop to the (11) element of the neutrino mass matrix (neglecting the tree level contribution). The trilinear R-parity violating couplings involved in these loop contributions are λ_{133} and λ'_{133}, which are identified with the tau and the bottom Yukawa couplings. The other parameters which play a crucial role in order to fit the (11) element of the neutrino mass matrix are $\tan\beta$, $m_{3/2}$ and $m^2_{\tilde{b}}$ (assuming that the stau-tau loop contribution is smaller than the other loop contributions). However, for a fixed value of $\tan\beta$ the trilinear couplings λ_{133} and λ'_{133} are fixed and thus this leaves us with only two parameters ($m_{3/2}$ and $m^2_{\tilde{b}}$) in terms of which $(m_\nu)_{11}$ can be fitted. Figure 9 presents the contour plots of $(m_\nu)_{11}$ in the ($m_{3/2}$–$m_{\tilde{b}}$) plane. Here the blue-dotted line corresponds to the maximum value of

JHEP01(2014)101

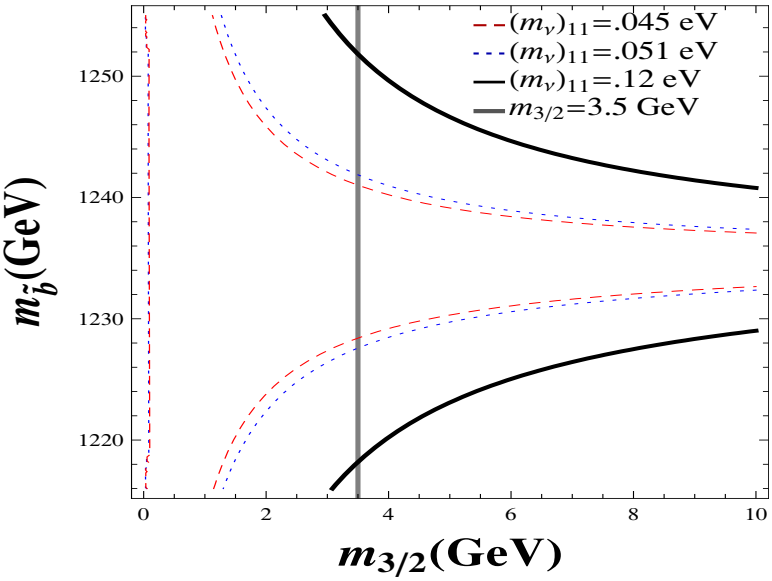

Figure 9. Contours of $(m_\nu)_{11}$ in the $(m_{3/2}$–$m_{\tilde{b}})$ plane for inverted hierarchy and $\tan\beta = 10$. See text for details.

$(m_\nu)_{11}$ whereas the red-dashed line corresponds to the minimum value of $(m_\nu)_{11}$. These maximum and minimum values are obtained by varying the oscillation parameters within the 3σ range. Moreover, we also draw a third contour (the black-bold line) which represents the upper bound on $(m_\nu)_{11}$ as obtained by the neutrinoless double beta decay experiments kamLAND-Zen and EXO-200 [87, 88].

In order to produce this figure we fixed all the other parameters at values corresponding to BP-4. The grey line represents a gravitino mass of 3.5 GeV. On the right hand side of this grey vertical line the mass of the sterile neutrino is ≥ 0.41 keV. Moreover, this plot shows the allowed range of sbottom mass, required to fit $(m_\nu)_{11}$ for fixed values of $\tan\beta$ and $m_{3/2}$. For example, we see that for $\tan\beta = 10$, $m_{3/2} = 3.5$ GeV, the sbottom mass is allowed in the range (1228–1242) GeV. For larger values of $\tan\beta$ the allowed range of $m_{\tilde{b}}$ increases.

Bounds on the trilinear RPV couplings for inverted hierarchy. By varying the neutrino oscillation parameters within their 3σ allowed ranges we can get maximum and minimum values for different neutrino mass matrix elements. These allowed ranges of neutrino mass matrix elements can be translated into a lower and an upper bound on different trilinear R-parity violating couplings involved. With the choice of other parameters as presented in BP-4, we present in table 4 the bounds on λ and λ' type couplings as functions $m_{\tilde{b}}$ and $m_{3/2}$ for a particular value of $\tan\beta = 10$. Note that these bounds are independent of the choices of other parameters shown in different benchmark points because they are calculated from the neutrino mass matrix elements which get contributions only from the one loop corrections.

JHEP01(2014)101

Couplings	Bounds for BP-4	Existing bounds
$\lvert\lambda'_{233}\rvert$	$(2.37\times10^{-7}-1.03\times10^{-6})\left(\frac{m_{\tilde{b}}}{100\ \text{GeV}}\right)^2\left(\frac{10\ \text{GeV}}{m_{3/2}}\right)$	$6.8\times10^{-3}\cos\beta$
$\lvert\lambda'_{333}\rvert$	$(2.84\times10^{-7}-1.04\times10^{-6})\left(\frac{m_{\tilde{b}}}{100\ \text{GeV}}\right)^2\left(\frac{10\ \text{GeV}}{m_{3/2}}\right)$	$1.305\cos\beta$
$\lvert\lambda'_{232}\lambda'_{223}\rvert$	$(2.11-4.3)\times10^{-5}\left(\frac{m_{\tilde{b}}}{100\ \text{GeV}}\right)^2\left(\frac{10\ \text{GeV}}{m_{3/2}}\right)$	$(2\times10^{-3})\cos^2\beta\,(\tilde{\nu}_{L_2}\tilde{u}_{L_3})^2$
$\lvert\lambda'_{223}\lambda'_{332}\rvert$	$(2.82-3.34)\times10^{-5}\left(\frac{m_{\tilde{b}}}{100\ \text{GeV}}\right)^2\left(\frac{10\ \text{GeV}}{m_{3/2}}\right)$	—
$\lvert\lambda'_{323}\lambda'_{332}\rvert$	$(2.38-4.64)\times10^{-5}\left(\frac{m_{\tilde{b}}}{100\ \text{GeV}}\right)^2\left(\frac{10\ \text{GeV}}{m_{3/2}}\right)$	—

Table 4. Bounds on λ_{ijk} and $\lambda^{'}_{ijk}$ couplings for $\tan\beta = 10$ and for inverted hierarchy.

9.2 Neutrino masses and mixing: normal hierarchy

In the case of normal hierarchy best-fit values of the neutrino oscillation parameters are given as [5] $\Delta m^2_{21} = 7.62\times10^{-5}\,\text{eV}^2$, $|\Delta m^2_{31}| = 2.55\times10^{-3}\,\text{eV}^2$ and the three mixing angles are $\theta_{12} = 34.4^\circ$, $\theta_{23} = 51.5^\circ$ and $\theta_{13} = 9.1^\circ$. With these values and assuming that $m_1 = 0$, $m_2^2 = \Delta m^2_{21}$ and $m_3^2 = |\Delta m^2_{31}|$ the neutrino mass matrix in the case of normal hierarchy turns out to be

$$m_\nu^{NH} = \begin{pmatrix} 0.0039 & 0.0082 & 0.0014 \\ 0.0082 & 0.0318 & 0.021 \\ 0.0014 & 0.021 & 0.023 \end{pmatrix}. \tag{9.4}$$

Figure 10 presents the contour of $(m_\nu)_{11}$ in the $(m_{3/2}$–$m_{\tilde{b}})$ plane in the case of normal hierarchy. Here the blue-dotted line corresponds to the maximum value of $(m_\nu)_{11} = 0.005\,\text{eV}$ whereas the red-dashed line corresponds to the minimum value of $(m_\nu)_{11} = 0.003\,\text{eV}$. Once again these maximum and minimum values are obtained by varying the oscillation parameters within their 3σ range.

The right side of the 3.5 GeV gravitino mass line can produce a keV sterile neutrino warm dark matter with a mass greater than 0.41 keV. The values of other parameters correspond to BP-4. Here we have chosen a small $\lambda_S = 10^{-4}$, which requires heavy stops to produce a $\sim 125\,\text{GeV}$ Higgs boson. Looking at this figure one can also see the range of sbottom mass required to fit the value of $(m_\nu)_{11}$ for a fixed value of $\tan\beta$ and $m_{3/2}$. If we take a large value of λ_s, then the $m_{\tilde{b}}$ mass range changes slightly but the essential feature remains the same.

Bounds on the trilinear RPV couplings for normal hierarchy. One can also constrain the trilinear R-parity violating couplings in the case of normal hierarchy after analyzing the other elements of the neutrino mass matrix in the light of neutrino data. The resulting bounds are shown in table 5. Bounds on trilinear R-parity violating couplings from various other studies can be found in [89–100].

10 Case with large neutrino Yukawa coupling

While discussing the sum rules in the scalar sector, we observed that the lightest Higgs boson mass receives an additional tree level contribution due to the presence of the neutrino

JHEP01(2014)101

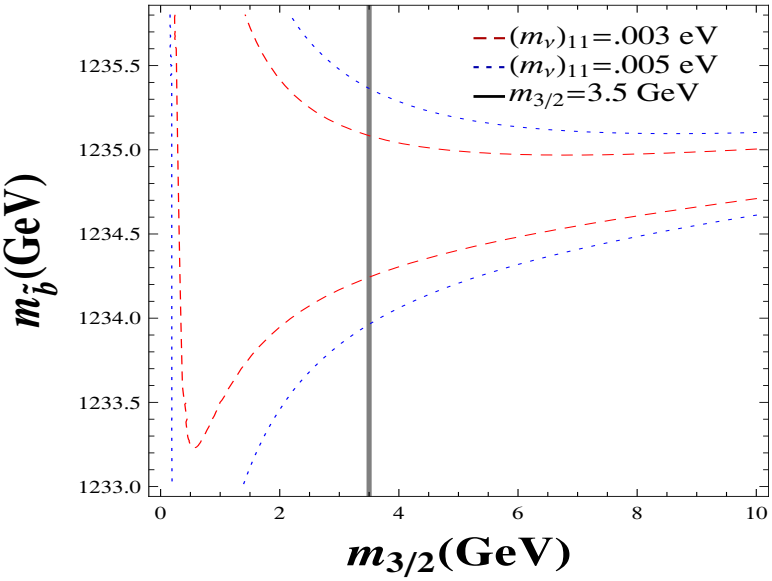

Figure 10. Contours of $(m_\nu)_{11}$ in the $(m_{3/2}$–$m_{\tilde{b}})$ plane for normal hierarchy case and $\tan\beta = 10$.

Couplings	Bounds for BP-4	Existing Constraints
$\lvert\lambda'_{233}\rvert$	$(8.07\times10^{-7} - 1.2\times10^{-6})\left(\frac{m_{\tilde{b}}}{100\text{ GeV}}\right)^2\left(\frac{10\text{ GeV}}{m_{3/2}}\right)$	$6.8\times10^{-3}\cos\beta$
$\lvert\lambda'_{333}\rvert$	$(3.74\times10^{-8} - 6.11\times10^{-7})\left(\frac{m_{\tilde{b}}}{100\text{ GeV}}\right)^2\left(\frac{10\text{ GeV}}{m_{3/2}}\right)$	$1.305\cos\beta$
$\lvert\lambda'_{232}\lambda'_{223}\rvert$	$(2.5-4.7)\times10^{-5}\left(\frac{m_{\tilde{b}}}{100\text{ GeV}}\right)^2\left(\frac{10\text{ GeV}}{m_{3/2}}\right)$	$(2\times10^{-3})\cos^2\beta\,(\tilde{\nu}_{L_2}\tilde{u}_{L_3})^2$
$\lvert\lambda'_{223}\lambda'_{332}\rvert$	$(2.4-3.0)\times10^{-5}\left(\frac{m_{\tilde{b}}}{100\text{ GeV}}\right)^2\left(\frac{10\text{ GeV}}{m_{3/2}}\right)$	—
$\lvert\lambda'_{323}\lambda'_{332}\rvert$	$(2.5-4.69)\times10^{-5}\left(\frac{m_{\tilde{b}}}{100\text{ GeV}}\right)^2\left(\frac{10\text{ GeV}}{m_{3/2}}\right)$	—

Table 5. Bounds on λ_{ijk} and $\lambda^{'}_{ijk}$ couplings for $\tan\beta = 10$ and for normal hierarchy.

Yukawa term $f\hat{H}_u\hat{L}_a\hat{N}^c$ in the superpotential. In the minimal supersymmetric standard model (MSSM) one requires a very large loop correction in order to fit the Higgs boson mass in the range of (123–127) GeV [101]. In the next-to-minimal supersymmetric model (NMSSM), the μ term is dynamically generated through a $\lambda_S S H_u H_d$ term in the superpotential and the tree level Higgs boson mass receives a correction proportional to λ_S^2 [101]. Similarly in the singlet-triplet extension of the MSSM, a tree level correction to the Higgs boson mass proportional to λ_S^2 and λ_T^2 is obtained [42]. However, in this model these tree level contributions to the lightest Higgs boson mass are absent but because of the presence of the neutrino Yukawa coupling f an additional contribution $(\Delta m_h^2)_{\text{tree}} = f^2v^2\sin^2 2\beta$ is obtained. In figure 11 we show the variation of the lightest Higgs boson mass in this model as a function of $\tan\beta$. We can observe from this figure that for a low value of $\tan\beta$ the Higgs boson mass of ~ 125 GeV can be achieved with $f = 0.9$, even at the tree level. Moreover, we find that $m_{\tilde{t}_1} = m_{\tilde{t}_2} = 500$ GeV is sufficient enough to provide the correct Higgs boson mass through radiative corrections for a slightly larger value of $\tan\beta$.

In this case the parameter M_R, included in the superpotential as $M_R N^c S$, is very large and thus the sterile neutrino becomes very heavy (see eq. (4.6)). In such a situation the lightest neutralino with a large bino component becomes the LSP with a very small

JHEP01(2014)101

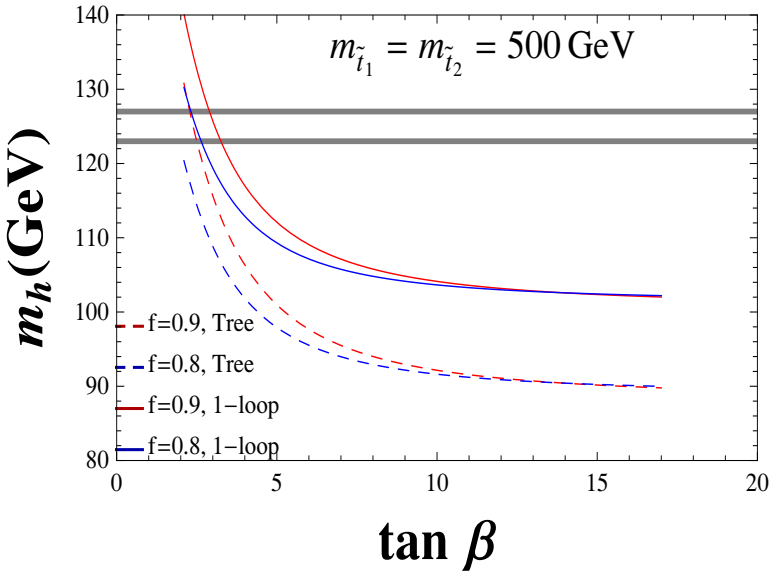

Figure 11. The variation of the lightest Higgs boson mass with $\tan\beta$. The dashed lines represent the Higgs boson mass at the tree level and the continuous lines represent the Higgs boson mass after radiative correction is added for a stop mass of 500 GeV. Here red corresponds to $f = 0.9$ whereas blue corresponds to $f = 0.8$.

mass of a few hundred MeV. The mass of the LSP is essentially controlled by the R-symmetry violating Majorana gaugino mass parameter M_1. We show the benchmark points corresponding to the large f scenario in table 6, where a tree level neutrino mass of 0.049 eV and a lightest neutralino mass of 167 MeV are obtained. Several studies can be found in the literature [102–106] concerning very light neutralinos. These include non universal gaugino mass models and R-parity violation. In the context of NMSSM with R-parity conservation, a few hundred MeV bino-like lightest neutralino has been studied as a dark matter candidate and it has been shown that one can avoid the overproduction of such a light neutralino in the early universe through efficient annihilations [107].

However, in our case the MeV neutralino LSP can decay through R-parity violating channels. Note, that in this case the gravitino with a mass of ~ 10 GeV decays mainly to the lightest neutralino + photon final state and has a lifetime of $\sim 10^{12}$ sec. Such a gravitino will decay after the big-bang nucleosynthesis (BBN) producing an unacceptable amount of entropy. This conflicts with the predictions of BBN if one assumes the standard big-bang cosmology and results in a constraint on the gravitino mass to be $m_{3/2} > 10$ TeV [108]. However, this constraint on the gravitino mass can be avoided if one assumes that the universe had gone through an inflationary phase and in order to avoid the strong constraints obtained from the photo-dissociation of the light elements because of the radiative decay of the gravitino, one arrives at the upper bound on the reheating temperature of the universe $T_R \lesssim 10^6$ GeV [105, 109]. In this case the gravitino is a stable particle in the collider time scale. However, it cannot be a candidate for dark matter because of its small lifetime in the cosmological time scale. Implications of such a scenario in the context of collider studies and dark matter requires further investigations and we shall postpone this for a future work.

JHEP01(2014)101

Parameters	BP-7
M_1^D	800 GeV
M_2^D	580 GeV
$\tan\beta$	2.6
λ_S	10^{-5}
λ_T	$\lambda_S \tan\theta_W \sim 5.5 \times 10^{-6}$
μ	200 GeV
t_S	$(200)^3$
$\mathrm{b}\mu_L$	$-(200)^2$ $(\mathrm{GeV})^2$
m_S	7.39 TeV
m_T	7.7 TeV
v_S	0.5 GeV
v_T	0.1 GeV
f	0.9
M_R	7.4 TeV
$m_{\tilde{t}_1} = m_{\tilde{t}_2}$	500 GeV
b_S	1 TeV
b_T	1 TeV
$m_{3/2}$	20 GeV
m_h	125.5 GeV
$(m_\nu)_{\mathrm{Tree}}$	0.049 eV
$m^0_{\tilde{\chi}}$	167 MeV

Table 6. A benchmark point with large f and small λ_S and λ_T.

11 Conclusions and outlook

We have studied a supersymmetric model of neutrino masses and mixing with an $\mathrm{U}(1)_R$ symmetry and a single right handed neutrino superfield. In this model the R-symmetry is identified with lepton number in such a way that the lepton numbers of the standard model fermions are the same as their R-charges but with a negative sign. The neutral gauginos are Dirac fermions in this model and one needs to introduce additional chiral superfields in the adjoint representations of the gauge groups. The right-handed neutrino with an appropriate R-charge allows one to write down neutrino Yukawa interactions respecting the $\mathrm{U}(1)_R$ symmetry. After the electroweak symmetry breaking one of the sneutrinos (we choose it to be the electron sneutrino) develops a non-zero vacuum expectation value, which can be significant because it is not constrained by small neutrino masses. In the neutral fermion sector we have mixing among the neutralinos, the electron-neutrino and the right handed neutrino consistent with the R-symmetry and that results in a small Dirac neutrino mass at the tree level. The scalar sector of this model can accommodate a Higgs boson with $\sim 125\,\mathrm{GeV}$ mass. This can be achieved even at the tree level with the help of a large Dirac neutrino Yukawa coupling ($f \sim 1$) or including the one loop radiative corrections to the tree level mass of the Higgs boson. A very important property of this R-symmetric

JHEP01(2014)101

model is the existence of a subset of R-parity violating interactions in the superpotential parametrized by λ and λ' in the literature.

There are two massless active neutrinos at the tree level, which acquire non-zero masses through one-loop radiative corrections when small R-symmetry breaking effects are turned on through a small gravitino mass. In this work we confine ourselves in a situation where the breaking of R-symmetry is communicated to the visible sector through anomaly mediated supersymmetry breaking. This results in small Majorana gaugino masses as well as trilinear scalar couplings, which were zero in the R-conserving limit. Depending on the size of the R-symmetry breaking order parameter (gravitino mass $m_{3/2}$ in this case), one can either generate a pair of almost degenerate neutrinos forming a pseudo-Dirac neutrino or two distinct light Majorana neutrinos from the neutralino-neutrino mass matrix at the tree level. Our analysis shows that none of these situations can accommodate the results from LSND experiments with a possible neutrino mass eigenstate at $\sim 1.2\,\text{eV}$. On the other hand, there exists a possibility of having a Majorana sterile neutrino with a mass of the order of a few keV, which can be a good candidate for warm dark matter. A detail scan of our parameter space shows that there are allowed regions where the constraints on this keV dark matter coming from X-ray observations can be satisfied and this keV sterile neutrino can account for the dark matter relic density measured at the PLANCK and WMAP experiments. At the same time there exists an active neutrino acquiring a very small mass at the tree level. All these allowed points in the parameter space are consistent with a $\sim 125\,\text{GeV}$ light Higgs boson. We have also identified two distinct cases of heavy and light stop masses consistent with the Higgs boson mass, dark matter relic density constraint and a small tree level mass of the neutrino. The collider signatures of these two cases should be explored further which can possibly provide some testable predictions at the LHC. Because of the mixing in the neutralino, chargino and the scalar mass matrices the sparticles can have novel decay modes leading to interesting final states in pp collision and can be studied in a similar way as presented in ref. [17].

We investigate the light active neutrino sector and try to fit the three flavor global neutrino data by incorporating one loop radiative corrections to the (3×3) light neutrino mass matrix. We choose certain benchmark points for our numerical analysis and show that one can obtain bounds on the trilinear R-parity violating couplings in the superpotential from neutrino data as a function of the R-symmetry breaking order parameter ($m_{3/2}$). We further pay a special attention to the situation with a large Dirac neutrino Yukawa coupling f and demonstrate that a large f can induce additional tree level contribution to the lightest Higgs boson mass to be consistent with the Higgs boson mass measurement at the LHC experiments. Even with such a large value of f, a small Majorana mass for the light active neutrino can be generated at the tree level. A very interesting feature of this scenario is the existence of a few hundred MeV lightest neutralino LSP with a substantial bino component. In this R-parity violating scenario, this MeV lightest neutralino LSP can decay into final states involving standard model fermions and can avoid the constraints on such a light MeV neutralino from its overproduction in the early universe. The gravitino is the NLSP in this case with a mass $m_{3/2} \sim 10\,\text{GeV}$ and it is a stable particle in the collider time scale with a lifetime of $\sim 10^{12}$ sec. This is cosmologically consistent as long

JHEP01(2014)101

as the reheating temperature $T_R \lesssim 10^6\,\text{GeV}$. It would be really interesting to see the phenomenological and cosmological implications of this MeV neutralino scenario in detail, and in particular, at the LHC. However, such a dedicated analysis is beyond the scope of this paper.

Acknowledgments

SC would like to thank the Council of Scientific and Industrial Research, Govt. of India for the financial support received as a Senior Research Fellow. He also thanks K. Huitu, J. Maalampi, K. Kainulainen, P. Bandyopadhyay, S. Di Chiara and Subhadeep Mondal for many useful comments and suggestions.

References

[1] ATLAS collaboration, *Observation of a new particle in the search for the standard model Higgs boson with the ATLAS detector at the LHC*, *Phys. Lett.* **B 716** (2012) 1 [arXiv:1207.7214] [INSPIRE].

[2] CMS collaboration, *Observation of a new boson at a mass of* 125 *GeV with the CMS experiment at the LHC*, *Phys. Lett.* **B 716** (2012) 30 [arXiv:1207.7235] [INSPIRE].

[3] CMS collaboration, *Search for supersymmetry in hadronic final states with missing transverse energy using the variables α_T and b-quark multiplicity in pp collisions at* 8 *TeV*, *Eur. Phys. J.* **C 73** (2013) 2568 [arXiv:1303.2985] [INSPIRE].

[4] ATLAS collaboration, *Search for new phenomena in final states with large jet multiplicities and missing transverse momentum at $\sqrt{s} = 8$ TeV proton-proton collisions using the ATLAS experiment*, *JHEP* **10** (2013) 130 [arXiv:1308.1841] [INSPIRE].

[5] T. Schwetz, M. Tortola and J. Valle, *Global neutrino data and recent reactor fluxes: status of three-flavour oscillation parameters*, *New J. Phys.* **13** (2011) 063004 [arXiv:1103.0734] [INSPIRE].

[6] T. Schwetz, M. Tortola and J. Valle, *Where we are on θ_{13}: addendum to 'Global neutrino data and recent reactor fluxes: status of three-flavour oscillation parameters'*, *New J. Phys.* **13** (2011) 109401 [arXiv:1108.1376] [INSPIRE].

[7] M. Gonzalez-Garcia, M. Maltoni, J. Salvado and T. Schwetz, *Global fit to three neutrino mixing: critical look at present precision*, *JHEP* **12** (2012) 123 [arXiv:1209.3023] [INSPIRE].

[8] DAYA-BAY collaboration, F. An et al., *Observation of electron-antineutrino disappearance at Daya Bay*, *Phys. Rev. Lett.* **108** (2012) 171803 [arXiv:1203.1669] [INSPIRE].

[9] RENO collaboration, J. Ahn et al., *Observation of reactor electron antineutrino disappearance in the RENO experiment*, *Phys. Rev. Lett.* **108** (2012) 191802 [arXiv:1204.0626] [INSPIRE].

[10] Planck collaboration, P. Ade et al., *Planck 2013 results. XVI. Cosmological parameters*, arXiv:1303.5076 [INSPIRE].

[11] N. Jarosik et al., *Seven-year Wilkinson Microwave Anisotropy Probe (WMAP) Observations: sky maps, systematic errors and basic results*, *Astrophys. J. Suppl.* **192** (2011) 14 [arXiv:1001.4744] [INSPIRE].

[12] J.L. Feng, *Dark matter candidates from particle physics and methods of detection*, *Ann. Rev. Astron. Astrophys.* **48** (2010) 495 [arXiv:1003.0904] [INSPIRE].

[13] R. Barbier et al., *R-parity violating supersymmetry*, *Phys. Rept.* **420** (2005) 1 [hep-ph/0406039] [INSPIRE].

[14] C. Frugiuele and T. Gregoire, *Making the sneutrino a Higgs with a* $\mathrm{U}(1)_R$ *lepton number*, *Phys. Rev.* **D 85** (2012) 015016 [arXiv:1107.4634] [INSPIRE].

[15] E. Bertuzzo and C. Frugiuele, *Fitting neutrino physics with a* $\mathrm{U}(1)_R$ *lepton number*, *JHEP* **05** (2012) 100 [arXiv:1203.5340] [INSPIRE].

[16] C. Frugiuele, T. Gregoire, P. Kumar and E. Ponton, *'*$L = R$*' —* $\mathrm{U}(1)_R$ *as the origin of leptonic 'RPV'*, *JHEP* **03** (2013) 156 [arXiv:1210.0541] [INSPIRE].

[17] C. Frugiuele, T. Gregoire, P. Kumar and E. Ponton, *'*$L = R$*' —* $\mathrm{U}(1)_R$ *lepton number at the LHC*, *JHEP* **05** (2013) 012 [arXiv:1210.5257] [INSPIRE].

[18] F. Riva, C. Biggio and A. Pomarol, *Is the* 125 *GeV Higgs the superpartner of a neutrino?*, *JHEP* **02** (2013) 081 [arXiv:1211.4526] [INSPIRE].

[19] P. Fayet, *Supersymmetry and weak, electromagnetic and strong interactions*, *Phys. Lett.* **B 64** (1976) 159 [INSPIRE].

[20] L.J. Hall, *Alternative low-energy supersymmetry*, *Mod. Phys. Lett.* **A 5** (1990) 467 [INSPIRE].

[21] L. Hall and L. Randall, $\mathrm{U}(1)_R$ *symmetric supersymmetry*, *Nucl. Phys.* **B 352** (1991) 289 [INSPIRE].

[22] A.E. Nelson, N. Rius, V. Sanz and M. Ünsal, *The minimal supersymmetric model without a* μ *term*, *JHEP* **08** (2002) 039 [hep-ph/0206102] [INSPIRE].

[23] Z. Chacko, P.J. Fox and H. Murayama, *Localized supersoft supersymmetry breaking*, *Nucl. Phys.* **B 706** (2005) 53 [hep-ph/0406142] [INSPIRE].

[24] I. Jack and D. Jones, *Nonstandard soft supersymmetry breaking*, *Phys. Lett.* **B 457** (1999) 101 [hep-ph/9903365] [INSPIRE].

[25] K. Benakli and M.D. Goodsell, *Dirac gauginos in general gauge mediation*, *Nucl. Phys.* **B 816** (2009) 185 [arXiv:0811.4409] [INSPIRE].

[26] S.Y. Choi, M. Drees, A. Freitas and P.M. Zerwas, *Testing the Majorana nature of gluinos and neutralinos*, *Phys. Rev.* **D 78** (2008) 095007 [arXiv:0808.2410] [INSPIRE].

[27] A. Kumar, D. Tucker-Smith and N. Weiner, *Neutrino mass, sneutrino dark matter and signals of lepton flavor violation in the MRSSM*, *JHEP* **09** (2010) 111 [arXiv:0910.2475] [INSPIRE].

[28] B.A. Dobrescu and P.J. Fox, *Uplifted supersymmetric Higgs region*, *Eur. Phys. J.* **C 70** (2010) 263 [arXiv:1001.3147] [INSPIRE].

JHEP01(2014)101

[29] K. Benakli, *Dirac gauginos: a user manual*, *Fortsch. Phys.* **59** (2011) 1079 [arXiv:1106.1649] [INSPIRE].

[30] K. Benakli, M.D. Goodsell and F. Staub, *Dirac gauginos and the* 125 *GeV Higgs*, *JHEP* **06** (2013) 073 [arXiv:1211.0552] [INSPIRE].

[31] R. Davies and M. McCullough, *Small neutrino masses due to R-symmetry breaking for a small cosmological constant*, *Phys. Rev.* **D 86** (2012) 025014 [arXiv:1111.2361] [INSPIRE].

[32] C. Brust, A. Katz, S. Lawrence and R. Sundrum, *SUSY, the third generation and the LHC*, *JHEP* **03** (2012) 103 [arXiv:1110.6670] [INSPIRE].

[33] G.D. Kribs, E. Poppitz and N. Weiner, *Flavor in supersymmetry with an extended R-symmetry*, *Phys. Rev.* **D 78** (2008) 055010 [arXiv:0712.2039] [INSPIRE].

[34] P.J. Fox, A.E. Nelson and N. Weiner, *Dirac gaugino masses and supersoft supersymmetry breaking*, *JHEP* **08** (2002) 035 [hep-ph/0206096] [INSPIRE].

[35] K. Benakli, M.D. Goodsell and A.-K. Maier, *Generating μ and $B\mu$ in models with Dirac gauginos*, *Nucl. Phys.* **B 851** (2011) 445 [arXiv:1104.2695] [INSPIRE].

[36] W. Buchmüller, L. Covi, K. Hamaguchi, A. Ibarra and T. Yanagida, *Gravitino dark matter in R-parity breaking vacua*, *JHEP* **03** (2007) 037 [hep-ph/0702184] [INSPIRE].

[37] K.N. Abazajian, *Detection of dark matter decay in the X-ray*, arXiv:0903.2040 [INSPIRE].

[38] LSND collaboration, C. Athanassopoulos et al., *Evidence for anti-muon-neutrino $\rightarrow$ anti-electron-neutrino oscillations from the LSND experiment at LAMPF*, *Phys. Rev. Lett.* **77** (1996) 3082 [nucl-ex/9605003] [INSPIRE].

[39] LSND collaboration, C. Athanassopoulos et al., *Evidence for $\nu_\mu \rightarrow \nu_e$ neutrino oscillations from LSND*, *Phys. Rev. Lett.* **81** (1998) 1774 [nucl-ex/9709006] [INSPIRE].

[40] LSND collaboration, A. Aguilar-Arevalo et al., *Evidence for neutrino oscillations from the observation of anti-neutrino(electron) appearance in a anti-neutrino(muon) beam*, *Phys. Rev.* **D 64** (2001) 112007 [hep-ex/0104049] [INSPIRE].

[41] J. Espinosa and M. Quirós, *Higgs triplets in the supersymmetric standard model*, *Nucl. Phys.* **B 384** (1992) 113 [INSPIRE].

[42] T. Basak and S. Mohanty, *Triplet-singlet extension of the MSSM with a* 125 *GeV Higgs and dark matter*, *Phys. Rev.* **D 86** (2012) 075031 [arXiv:1204.6592] [INSPIRE].

[43] N. Arkani-Hamed, S. Dimopoulos, G. Giudice and A. Romanino, *Aspects of split supersymmetry*, *Nucl. Phys.* **B 709** (2005) 3 [hep-ph/0409232] [INSPIRE].

[44] M.D. Goodsell, *Two-loop RGEs with Dirac gaugino masses*, *JHEP* **01** (2013) 066 [arXiv:1206.6697] [INSPIRE].

[45] G. Bélanger, K. Benakli, M. Goodsell, C. Moura and A. Pukhov, *Dark matter with Dirac and Majorana gaugino masses*, *JCAP* **08** (2009) 027 [arXiv:0905.1043] [INSPIRE].

[46] PARTICLE DATA GROUP collaboration, J. Beringer et al., *Review of particle physics*, *Phys. Rev.* **D 86** (2012) 010001 [INSPIRE].

[47] I. Simonsen, *A review of minimal supersymmetric electroweak theory*, hep-ph/9506369 [INSPIRE].

[48] Y. Morita, H. Nakano and T. Shimomura, *Neutrino mass and proton decay in a $\mathrm{U}(1)_R$ symmetric model*, *PTEP* **2013** (2013) 053B02 [arXiv:1212.4304] [INSPIRE].

JHEP01(2014)101

[49] S.P. Martin, *A supersymmetry primer*, in *Perspectives on supersymmetry II*, G.L. Kane ed. World Scientific, Singapore (2010), hep-ph/9709356 [INSPIRE].

[50] T. Gherghetta, G.F. Giudice and J.D. Wells, *Phenomenological consequences of supersymmetry with anomaly induced masses*, *Nucl. Phys.* **B 559** (1999) 27 [hep-ph/9904378] [INSPIRE].

[51] D.K. Ghosh, A. Kundu, P. Roy and S. Roy, *Characteristic wino signals in a linear collider from anomaly mediated supersymmetry breaking*, *Phys. Rev.* **D 64** (2001) 115001 [hep-ph/0104217] [INSPIRE].

[52] E.K. Akhmedov, *Neutrino physics*, hep-ph/0001264 [INSPIRE].

[53] M. Ghosh, S. Goswami and S. Gupta, *Two zero mass matrices and sterile neutrinos*, *JHEP* **04** (2013) 103 [arXiv:1211.0118] [INSPIRE].

[54] Y. Zhang, *Majorana neutrino mass matrices with three texture zeros and the sterile neutrino*, *Phys. Rev.* **D 87** (2013) 053020 [arXiv:1301.7302] [INSPIRE].

[55] M. Ghosh, S. Goswami, S. Gupta and C. Kim, *Implication of a vanishing element in* $3+1$ *Scenario*, *Phys. Rev.* **D 88** (2013) 033009 [arXiv:1305.0180] [INSPIRE].

[56] F. Bezrukov, H. Hettmansperger and M. Lindner, *keV sterile neutrino dark matter in gauge extensions of the standard model*, *Phys. Rev.* **D 81** (2010) 085032 [arXiv:0912.4415] [INSPIRE].

[57] M. Nemevšek, G. Senjanović and Y. Zhang, *Warm dark matter in low scale left-right theory*, *JCAP* **07** (2012) 006 [arXiv:1205.0844] [INSPIRE].

[58] Y. Grossman and D.J. Robinson, *Composite Dirac neutrinos*, *JHEP* **01** (2011) 132 [arXiv:1009.2781] [INSPIRE].

[59] D.J. Robinson and Y. Tsai, *KeV warm dark matter and composite neutrinos*, *JHEP* **08** (2012) 161 [arXiv:1205.0569] [INSPIRE].

[60] N.A. Ky and N.T.H. Van, *Scalar sextet in the* 331 *model with right-handed neutrinos*, *Phys. Rev.* **D 72** (2005) 115017 [hep-ph/0512096] [INSPIRE].

[61] D.N. Dinh, N.A. Ky, N.T. Van and P.Q. Van, *Model of neutrino effective masses*, *Phys. Rev.* **D 74** (2006) 077701 [INSPIRE].

[62] A. Merle and V. Niro, *Deriving Models for keV sterile Neutrino Dark Matter with the Froggatt-Nielsen mechanism*, *JCAP* **07** (2011) 023 [arXiv:1105.5136] [INSPIRE].

[63] A. Merle, *keV neutrino model building*, *Int. J. Mod. Phys.* **D 22** (2013) 1330020 [arXiv:1302.2625] [INSPIRE].

[64] A. Kusenko, *Sterile neutrinos: the dark side of the light fermions*, *Phys. Rept.* **481** (2009) 1 [arXiv:0906.2968] [INSPIRE].

[65] K. Abazajian et al., *Light sterile neutrinos: a white paper*, arXiv:1204.5379 [INSPIRE].

[66] K. Abazajian, G.M. Fuller and W.H. Tucker, *Direct detection of warm dark matter in the X-ray*, *Astrophys. J.* **562** (2001) 593 [astro-ph/0106002] [INSPIRE].

[67] A. Boyarsky, A. Neronov, O. Ruchayskiy, M. Shaposhnikov and I. Tkachev, *Where to find a dark matter sterile neutrino?*, *Phys. Rev. Lett.* **97** (2006) 261302 [astro-ph/0603660] [INSPIRE].

JHEP01(2014)101

[68] A. Boyarsky, A. Neronov, O. Ruchayskiy and M. Shaposhnikov, *Restrictions on parameters of sterile neutrino dark matter from observations of galaxy clusters*, *Phys. Rev.* **D 74** (2006) 103506 [astro-ph/0603368] [INSPIRE].

[69] M. Loewenstein, A. Kusenko and P.L. Biermann, *New limits on sterile neutrinos from Suzaku observations of the Ursa Minor dwarf spheroidal galaxy*, *Astrophys. J.* **700** (2009) 426 [arXiv:0812.2710] [INSPIRE].

[70] S. Riemer-Sorensen, K. Pedersen, S.H. Hansen and H. Dahle, *Probing the nature of dark matter with cosmic X-rays: constraints from dark blobs and grating spectra of galaxy clusters*, *Phys. Rev.* **D 76** (2007) 043524 [astro-ph/0610034] [INSPIRE].

[71] R. Hundi and S. Roy, *Constraints on composite Dirac neutrinos from observations of galaxy clusters*, *Phys. Lett.* **B 702** (2011) 228 [arXiv:1105.0291] [INSPIRE].

[72] A. Boyarsky, O. Ruchayskiy and M. Shaposhnikov, *The role of sterile neutrinos in cosmology and astrophysics*, *Ann. Rev. Nucl. Part. Sci.* **59** (2009) 191 [arXiv:0901.0011] [INSPIRE].

[73] S. Dodelson and L.M. Widrow, *Sterile-neutrinos as dark matter*, *Phys. Rev. Lett.* **72** (1994) 17 [hep-ph/9303287] [INSPIRE].

[74] X.-D. Shi and G.M. Fuller, *A new dark matter candidate: nonthermal sterile neutrinos*, *Phys. Rev. Lett.* **82** (1999) 2832 [astro-ph/9810076] [INSPIRE].

[75] A. Kusenko, *Sterile neutrinos, dark matter and the pulsar velocities in models with a Higgs singlet*, *Phys. Rev. Lett.* **97** (2006) 241301 [hep-ph/0609081] [INSPIRE].

[76] K. Petraki and A. Kusenko, *Dark-matter sterile neutrinos in models with a gauge singlet in the Higgs sector*, *Phys. Rev.* **D 77** (2008) 065014 [arXiv:0711.4646] [INSPIRE].

[77] A. Falkowski, J.T. Ruderman and T. Volansky, *Asymmetric dark matter from leptogenesis*, *JHEP* **05** (2011) 106 [arXiv:1101.4936] [INSPIRE].

[78] A. Merle, V. Niro and D. Schmidt, *New production mechanism for keV sterile neutrino dark matter by decays of frozen-in scalars*, arXiv:1306.3996 [INSPIRE].

[79] A. Boyarsky, O. Ruchayskiy and D. Iakubovskyi, *A lower bound on the mass of dark matter particles*, *JCAP* **03** (2009) 005 [arXiv:0808.3902] [INSPIRE].

[80] D. Gorbunov, A. Khmelnitsky and V. Rubakov, *Constraining sterile neutrino dark matter by phase-space density observations*, *JCAP* **10** (2008) 041 [arXiv:0808.3910] [INSPIRE].

[81] A. Boyarsky, D. Iakubovskyi and O. Ruchayskiy, *Next decade of sterile neutrino studies*, *Phys. Dark Univ.* **1** (2012) 136 [arXiv:1306.4954] [INSPIRE].

[82] U. Seljak, A. Makarov, P. McDonald and H. Trac, *Can sterile neutrinos be the dark matter?*, *Phys. Rev. Lett.* **97** (2006) 191303 [astro-ph/0602430] [INSPIRE].

[83] A. Boyarsky, J. Lesgourgues, O. Ruchayskiy and M. Viel, *Lyman-α constraints on warm and on warm-plus-cold dark matter models*, *JCAP* **05** (2009) 012 [arXiv:0812.0010] [INSPIRE].

[84] Y. Grossman and H.E. Haber, *(S)neutrino properties in R-parity violating supersymmetry. 1. CP conserving phenomena*, *Phys. Rev.* **D 59** (1999) 093008 [hep-ph/9810536] [INSPIRE].

[85] S. Davidson and M. Losada, *Neutrino masses in the R(p) violating MSSM*, *JHEP* **05** (2000) 021 [hep-ph/0005080] [INSPIRE].

JHEP01(2014)101

[86] S. Davidson and M. Losada, *Basis independent neutrino masses in the $R(p)$ violating MSSM*, *Phys. Rev.* **D 65** (2002) 075025 [hep-ph/0010325] [INSPIRE].

[87] KAMLAND-ZEN collaboration, A. Gando et al., *Limit on Neutrinoless $\beta\beta$ Decay of Xe-136 from the First Phase of KamLAND-Zen and Comparison with the Positive Claim in Ge-76*, *Phys. Rev. Lett.* **110** (2013) 062502 [arXiv:1211.3863] [INSPIRE].

[88] EXO collaboration, M. Auger et al., *Search for neutrinoless double-beta decay in ^{136}Xe with EXO-200*, *Phys. Rev. Lett.* **109** (2012) 032505 [arXiv:1205.5608] [INSPIRE].

[89] H. Dreiner, K. Nickel, F. Staub and A. Vicente, *New bounds on trilinear R-parity violation from lepton flavor violating observables*, *Phys. Rev.* **D 86** (2012) 015003 [arXiv:1204.5925] [INSPIRE].

[90] H. Dreiner, M. Krämer and B. O'Leary, *Bounds on R-parity violating supersymmetric couplings from leptonic and semi-leptonic meson decays*, *Phys. Rev.* **D 75** (2007) 114016 [hep-ph/0612278] [INSPIRE].

[91] H. Dreiner, M. Hanussek and S. Grab, *Bounds on R-parity violating couplings at the grand unification scale from neutrino masses*, *Phys. Rev.* **D 82** (2010) 055027 [arXiv:1005.3309] [INSPIRE].

[92] J.P. Saha and A. Kundu, *Constraints on R parity violating supersymmetry from leptonic and semileptonic τ, B_d and B_s decays*, *Phys. Rev.* **D 66** (2002) 054021 [hep-ph/0205046] [INSPIRE].

[93] J.P. Saha and A. Kundu, *Reevaluating bounds on flavor changing neutral current parameters in R parity conserving and R parity violating supersymmetry from B^0-$\bar{B}^0$ mixing*, *Phys. Rev.* **D 69** (2004) 016004 [hep-ph/0307259] [INSPIRE].

[94] A. Kundu and J.P. Saha, *Constraints on R-parity violating supersymmetry from neutral meson mixing*, *Phys. Rev.* **D 70** (2004) 096002 [hep-ph/0403154] [INSPIRE].

[95] A. de Gouvêa, S. Lola and K. Tobe, *Lepton flavor violation in supersymmetric models with trilinear R-parity violation*, *Phys. Rev.* **D 63** (2001) 035004 [hep-ph/0008085] [INSPIRE].

[96] M. Chaichian and K. Huitu, *Constraints on R-parity violating interactions from $\mu \to e\gamma$*, *Phys. Lett.* **B 384** (1996) 157 [hep-ph/9603412] [INSPIRE].

[97] K. Huitu, J. Maalampi, M. Raidal and A. Santamaria, *New constraints on R-parity violation from μe conversion in nuclei*, *Phys. Lett.* **B 430** (1998) 355 [hep-ph/9712249] [INSPIRE].

[98] G. Bhattacharyya, J.R. Ellis and K. Sridhar, *New LEP constraints on some supersymmetric Yukawa interactions that violate R-parity*, *Mod. Phys. Lett.* **A 10** (1995) 1583 [hep-ph/9503264] [INSPIRE].

[99] K. Agashe and M. Graesser, *R-parity violation in flavor changing neutral current processes and top quark decays*, *Phys. Rev.* **D 54** (1996) 4445 [hep-ph/9510439] [INSPIRE].

[100] A. Abada and M. Losada, *Constraints on both bilinear and trilinear R-parity violating couplings from neutrino laboratories and astrophysics data*, *Phys. Lett.* **B 492** (2000) 310 [hep-ph/0007041] [INSPIRE].

[101] L.J. Hall, D. Pinner and J.T. Ruderman, *A natural SUSY Higgs near 126 GeV*, *JHEP* **04** (2012) 131 [arXiv:1112.2703] [INSPIRE].

[102] H.K. Dreiner et al., *Mass bounds on a very light neutralino*, *Eur. Phys. J.* **C 62** (2009) 547 [arXiv:0901.3485] [INSPIRE].

JHEP01(2014)101

[103] L. Calibbi, J.M. Lindert, T. Ota and Y. Takanishi, *Cornering light neutralino dark matter at the LHC*, *JHEP* **10** (2013) 132 [arXiv:1307.4119] [INSPIRE].

[104] H.K. Dreiner, J.S. Kim and O. Lebedev, *First LHC constraints on neutralinos*, *Phys. Lett.* **B 715** (2012) 199 [arXiv:1206.3096] [INSPIRE].

[105] H.K. Dreiner, M. Hanussek, J.S. Kim and S. Sarkar, *Gravitino cosmology with a very light neutralino*, *Phys. Rev.* **D 85** (2012) 065027 [arXiv:1111.5715] [INSPIRE].

[106] D. Choudhury, H.K. Dreiner, P. Richardson and S. Sarkar, *A supersymmetric solution to the KARMEN time anomaly*, *Phys. Rev.* **D 61** (2000) 095009 [hep-ph/9911365] [INSPIRE].

[107] J.F. Gunion, D. Hooper and B. McElrath, *Light neutralino dark matter in the NMSSM*, *Phys. Rev.* **D 73** (2006) 015011 [hep-ph/0509024] [INSPIRE].

[108] S. Weinberg, *Cosmological constraints on the scale of supersymmetry breaking*, *Phys. Rev. Lett.* **48** (1982) 1303 [INSPIRE].

[109] M. Kawasaki and T. Moroi, *Gravitino production in the inflationary universe and the effects on big bang nucleosynthesis*, *Prog. Theor. Phys.* **93** (1995) 879 [hep-ph/9403364] [INSPIRE].

JHEP01(2014)101